The authors did a good job trying to improve the quality and answer the reviewers questions. That said I still see some major issue that prevent the publication of this article:

1) I still strongly think that the CO2 part of the paper is minor and shadowing the interesting analysis on water. The authors refer to CO2 partitioning that is not discussed in the paper (just an equation, already published, is applied and no gapfilling) and also the very important link between C and H2O is however not addressed in the paper. So I still think that the CO2 part is just marginal (and with issues, see below)

2) In the Section 2.4.1 it is still not clear if the LRC is parameterized using all the data or only data with ustar above the threshold. In the first case this is wrong, because these data are known to be underestimated, in the second case the method would be not any more independent by FVF. However as stated above I suggest to remove this section and may be write a separate paper on CO2 where all these aspects are analysed. In fact the overall discussion is in my opinion not robust enough, ignoring uncertainty (are they really different? Did you check the overall uncertainty?) and proposing a method that removes a lot of data (see P9, L16-17) so increasing the uncertainty in particular as function of the gapfilling method used. Also it looks like there is still confusion on the ustar method and advection: working or not working ustar filtering was proposed and developed for advection and hilly terrains, saying that is not appropriate is wrong. May be not sufficient in some cases but again this needs to be shown and discussed.

Response (comments 1 and 2): The CO_2 flux part of the manuscript was deleted as suggested.

3) I still think that the method should be part of a real validation and not a comparison between models or the use of measurements that are considered wrong in the paper (open path during rain). It means (referring to comments on Section 3.1.2 and answers) that the authors should find dataset were a close or closed path IRGA with heated tube is used and then apply the method developed to these data (e.g. adding artificial gaps) to validate the model and estimate the uncertainty. There are 600 sites in FLUXNET, a dataset like this is for sure available.

Response: Recently, we conducted a closed-path IRGA for the one of the study sites (i.e., GDK) with the original open-path EC system. We conducted the further evaluation using the data from the closed-path EC system. As we expected, the data retrieval rate under wet canopy condition of the closed-path EC system was 50% higher than that of the open-path EC system. However, there were still missing data for the considerable period despite the closed-path gas analyzer was conducted. The missing was mainly caused by the malfunction of the sonic anemometer and the unsatisfactory conditions for EC measurement (e.g., nonstationary and unfavorable turbulent developed conditions). Unlikely to photosynthesis and transpiration, wet canopy evaporation is strongly connected to the wet canopy evaporation which occurred in the previous time step (i.e., the wet canopy evaporation in the previous time step determines the intercepted canopy water. The model is a numerical model, not an analytical model). Because of such reasons, it is challengeable to validate (and estimate the uncertainty) the method as suggested (i.e., adding artificial gaps and gap-filling). Instead of that, we conducted the comparison between the model result and the observation from the closed-path EC system. The results of the error assessment were similar to those from the comparison between the model result and the observation from the open-path EC system. We added those results in the Appendix C.

The wet canopy evaporation occurs during and following rain events. The both, the open-path EC system and closed-path system, can measure some (NOT all) of the wet canopy evaporation. The latter has not only the advantage but also the disadvantage i.e., more robust under wet canopy condition (resulting higher data retrieval rate) and the underestimation due to tube attenuation in high RH condition. Additionally, there is no sonic anemometer which can measure perfectly and continuously during rain events (it also fails when the transducer probe is contaminated by rain drops).

Thus, we argue that (1) the dataset from a closed-path EC system is also not a perfect for assessing wet canopy evaporation; (2) the difference of data quality between the open-path and the closed-path is minor and only difference is the periods that instruments work properly; (3) an appropriate wet canopy evaporation gap-filling method is also necessitated in the case of the measurement using a closed path EC system, like the case of an open-path EC system. Related to the reviewer's suggestion, we also will do our efforts to measure evapotranspiration during and following rain events reliably and continuously and hope to estimate the uncertainty of our evapotranspiration gap-filling and partitioning methodology following the reviewer's suggestion as further study.

New ~~techniques for~~ gap-filling and partitioning __technique__ ~~of~~__for__ H_2O ~~and CO_2~~ eddy fluxes measured over forests ~~in complex mountainous terrain~~

Minseok Kang[1], Joon Kim[1,2,3,4], Bindu Malla Thakuri[2], Junghwa Chun[5], Chunho Cho[6]

[1]National Center for AgroMeteorology, Seoul, 08826, South Korea
[2]Program in Rural Systems Engineering, Department of Landscape Architecture & Rural Systems Engineering, Seoul National University, Seoul, 08826, South Korea
[3]Interdisciplinary Program in Agricultural & Forest Meteorology, Seoul National University, Seoul, 08826, South Korea
[4]Institute of Green Bio Science and Technology, Seoul National University Pyeongchang Campus, Pyeongchang, 25354, South Korea
[5]Department of Forest Conservation, National Institute of Forest Science, Seoul, 02455, South Korea
[6]National Institute of Meteorological Research, Seogwipo, 63568, South Korea

Correspondence to: Minseok Kang (ms-kang@ncam.kr)

Abstract. The continuous measurement of H_2O ~~and CO_2~~ fluxes using the eddy covariance (EC) technique is still challenging for forests ~~in complex terrain~~ because of large amounts of wet canopy evaporation (E_{WC}), which occur during and following rain events when the EC systems rarely work correctly~~, and the horizontal advection of CO_2 generated at night~~. We propose __a__ new ~~techniques for~~ gap-filling and partitioning __technique__ ~~of~~__for__ the H_2O ~~and CO_2~~ fluxes: ~~(1)__ a model-stats hybrid method (MSH) ~~and (2) a modified moving point test method (MPT$_m$)~~. ~~The former__It__ enables the recovery of the missing E_{WC} in the traditional gap-filling method and the partitioning of the evapotranspiration (ET) into transpiration and (wet canopy) evaporation. ~~The latter determines the friction velocity (u^*) threshold based on an iterative approach using moving windows for both time and u^*, thereby allowing not only the nighttime CO_2 flux correction and partitioning but also the assessment of the significance of the CO_2 drainage.~~ We tested and validated the~~se~~ new method~~s~~ using the datasets from two flux towers, which are located at forests in hilly and complex terrains. The MSH reasonably recovered the missing E_{WC} of 16 ~ 41 mm year^{-1} and separated it from the ET (14 ~ 23% of the annual ET). ~~The MPT$_m$ produced consistent carbon budgets using those from the previous research and diameter increment, while it has improved applicability.__ Additionally, we illustrated certain advantages of the proposed technique~~s~~, which enables us to understand better how ET responses to environmental changes and how the water cycle is connected to the carbon cycle in a forest ecosystem.

1 Introduction

Forest ecosystems share three properties that are significant in their interactions with the atmosphere. They are extensive, dense and tall, and thus produce sizable aerodynamic roughness and canopy storage for rainfall interception/evaporation (e.g.,

Shuttleworth, 1989). Since most of the flat terrains are used as agricultural lands and towns (or cities), substantial areas of forest exist in mountainous terrains where the fundamental assumptions of eddy covariance (EC) measurement (flat and homogeneous site, e.g., Baldocchi et al., 1988) are violated. These facts hinder the use of the EC method from assessing the net ecosystem exchanges (NEE) of H_2O and CO_2 in forests.

5   Considering that EC measures compound 'net' fluxes and its gaps are unavoidable, we commonly take great care for flux gap-filling and partitioning. Basically, the gap-filling and partitioning are a kind of interpolation and extrapolation based on that EC measurement has high temporal resolution and the bio-meteorological processes is a (repetitive) cycle ("redundancy" of data) (Papale et al., 2012). Generally, they consist of the following procedure: (1) setting a target flux (e.g., $CO_2/H_2O/CH_4$ fluxes, ecosystem respiration), (2) selecting drivers which control the target flux, (3) identifying relationships between the

10   (appropriate) target flux (which can represent true NEE) and the drivers, and (4) interpolating and extrapolating the relationships during a certain period when the relationship is maintained (e.g., Papale et al., 2012; Reichstein et al., 2012). In this context, the gap-filling and partitioning (including nighttime CO_2 flux correction) are coterminous with each other. The related scientific issue is determining/selecting the number and type of drivers, and the method and the time window size to identify the relationship. It depends on data availability, temporal scale of the process, and ecosystem state change. Those

15   processes require extra care for the measurement in complex mountainous terrain ~~as follows~~(e.g., van Gorsel et al., 2009; Kang et al., 2017).

1.1 Wet canopy evaporation: gap-filling and partitioning

Wet canopy evaporation (E_{WC}) is an evaporation of the intercepted water by the vegetation canopy during and following rain events, which may consist of a significant portion of evapotranspiration (ET). Over forests, it is hard to measure the E_{WC}

20   primarily due to the malfunction of an open-path EC system with rainfall. Although a closed-path system with an intake tube enables the E_{WC} measurement in the rain, the attenuation of the turbulent flow inside the tube acts as a low-pass filtering, which results in a significant underestimation of the E_{WC}. Furthermore, the attenuation domain expands with an increasing relative humidity (RH) from high frequency to medium frequency (e.g., Ibrom et al., 2007; Fratini et al., 2012). The closed-path EC system with the heated tube may be the most appropriate for measuring ET in the rain (e.g., Goodrich et al., 2016).

25   The missing (or low quality) data can be gap-filled using general gap-filling methods such as the marginal distribution sampling and artificial neural network (e.g., Reichstein et al., 2005; Papale and Valentini 2003). However, Kang et al. (2012) showed that, without a proper consideration of the E_{WC}, such gap-filled ET data under the wet canopy conditions are underestimated because the data used in such gap-filling are mostly collected dry or partially wet canopy condition when the EC systems work properly. The authors proposed an improved gap-filing method that is coupled with a simple canopy

30   (water) interception model.

The ET represents a combination of the E_{WC}, transpiration (T), and soil evaporation (E_S), which are controlled by different mechanisms and processes. Therefore, the partitioning of ET into the E_{WC}, T, and E_S is required to understand how ET is regulated by environmental changes and the how water cycle is connected to the carbon cycle in a forest ecosystem. For

2

these reasons, there have been many previous studies that partition ET using other supplementary measurements or empirical/process models (e.g., Wilson et al., 2001; Yepez et al., 2003; Daikoku et al., 2008; Stoy et al., 2006; Hu et al., 2009; Kang et al., 2009b). Despite the many previous studies on ET partitioning, most of them have focused on the partitioning of ET into the E_S (or direct evaporation, i.e., a sum of E_S and E_{WC}) and T. In the case of forest ecosystems with a dense canopy under a monsoon climate (e.g., East Asia, South Asia), the E_{WC} can play a greater role than the E_S. In this context, it is necessary to pay attention to the method described by Kang et al. (2012), which not only allows the proper estimation and gap-filling of the missing evaporation data under wet canopy conditions but also enables the partitioning of ET into the E_{WC} and T appropriately after certain modifications.

1.2 Nighttime CO_2 flux: correction for complex topography

In EC measurements over complex mountainous terrain, the nighttime CO_2 flux correction (i.e., eliminate the advection-affected data and fill the gaps) is one of the most important and challenging tasks. There are two types of widely used methods: (1) the friction velocity (u^*) filtering method, and (2) the advection based filtering method. The most commonly used method is the u^* filtering method that optimizes the parameters of the ecosystem respiration (RE) function using the observed nighttime CO_2 flux when u^* is greater than a threshold, (i.e., there is no dependency of the nighttime CO_2 flux on u^*) (e.g., Falge et al., 2001; Gu et al., 2005). The filtered data are replaced with the estimated data using ecosystem temperatures and the RE function with the optimized parameters (which is optimized using the remaining data). The u^* filtering method cannot be applied at sites where the u^* threshold cannot be determined and/or the drainage flow is generated during most of the night. Accordingly, an advection-based method was developed for hilly terrain sites that are affected by drainage flow (van Gorsel et al., 2007, 2008 and 2009). It omits most of the nighttime data and uses the observed CO_2 flux data near sunset when the nighttime advection has not yet affected to EC measurement. The nighttime correction is also important for the partitioning of NEE into gross primary productivity (GPP) and RE because the nighttime RE-temperature relationship is used to extrapolate the daytime RE (e.g., Reichstein et al., 2005).

The Gwangneung deciduous and coniferous forests sites in Korea, which are a part of Korea Flux Monitoring Network (KoFlux), are typical sites situated in hilly and complex terrains where these methods are difficult to apply appropriately because the CO_2 drainage generated earlier than the time assumed by the method. Kang et al. (2017) developed the site-specific quality control filter to exclude the data strongly affected by CO_2 advection. The filter identifies the observations that occur when a strong information flow toward the bottom of the slope exists in the dynamical process network of the observed multi-level CO_2 concentrations. This site-specific filter, which is qualitatively similar to the application of the traditional correction methods in a hybrid way, substantially reduced the disagreement among the three different conventional methods of nighttime CO_2 corrections. However, this method has low applicability because the measurements of CO_2 concentration profiles are required at two or more locations along the drainage, and a long-time series data is necessary to produce robust results. To overcome these shortcomings, we propose a hybrid of the u^* filtering and advection-based methods, which can be applied unconditionally, "*everywhere, all of the time.*"

3

In this study, we propose <u>a</u> new ~~techniques for~~ gap-filling and partitioning <u>technique</u> ~~o~~<u>for</u> the H_2O ~~and CO_2~~ fluxes measured over forests in complex mountainous terrain. First, we introduce a model-stats hybrid method, which can not only recover the missing E_{WC} in the general gap-filling method but also separate it from ET. Then, ~~an automated statistical method is~~

5 ~~introduced to determine the u^* threshold based on an iterative approach using a moving window of both time and u^* (i.e., the~~ ~~modified moving point test method). This method enables the determination of 'the significance of CO_2 drainage and the u^*~~ ~~threshold for the nighttime CO_2 flux correction and partitioning. W~~<u>w</u>e tested and validated these new methods using the datasets from the two flux towers, which are located in forests with hilly and complex terrains. Additionally, we illustrated certain advantages of the new technique~~s~~.

10 **2 Materials and Methods**

2.1 Study sites

In the Gwangneung National Arboretum, there are two eddy covariance flux towers: the Gwangneung deciduous forest located at the top of a hill (GDK; 37° 45' 25" N, 127° 09' 12" E) and the Gwangneung coniferous forest located at the bottom (GCK; 37° 44' 54" N, 127° 09' 45" E). Gwangneung has been protected to minimize human disturbance over the last

15 500 years. Both sites are located on complex, hilly catchment with a mean slope of 10 – 20°. The two towers are ~ 1.2 km apart, and the mean slope between them is ~ 6.2° (Moon et al., 2005). The east/west slopes are gentle, whereas the north/south slopes are steep in the catchment. The mountain-valley circulation is dominant wind regime in the sites (Hong et al., 2005; Yuan et al., 2007). Meteorological records from an automatic weather station ~ 1.6 km northeast of the tower for 1997-2016 show that annual mean air temperature is 10.1±0.6°C and the mean precipitation is 1,472±352 mm (National

20 Climate Data Service System, http://sts.kma.go.kr/). At the GDK site, the vegetation is dominated by an old natural forest of *Quercus* sp. and *Carpinus* sp. (80 – 200 years old) with a mean canopy height of ~ 18 m and a maximum leaf area index (LAI) of ~ 6 m^2 m^{-2} in June. Compared to the GDK site, the GCK site is in a lower area and is a flat, plantation forest with the dominant species of *Abies holophylla* (approximately 80 years old) with a mean canopy height of ~ 23 m and a maximum LAI of ~ 8 m^2 m^{-2} in June. Further descriptions of the sites can be found in Kim et al. (2006) and Kang et al. (2017).

25 **2.2 Measurements and data processing**

The H_2O and CO_2 fluxes have been measured since 2006 and 2007 at the GDK site and GCK site, respectively. At both sites, the EC system was used to measure the fluxes from a 40 m tower. The wind speed and temperature were measured with a three-dimensional sonic anemometer (Model CSAT3, Campbell Scientific Inc., Logan, Utah, USA), while the H_2O and CO_2 concentrations were measured with an open-path infrared gas analyzer (IRGA; Model LI-7500, LI-COR Inc., Lincoln,

30 Nebraska, USA) at both sites. Half-hourly ECs and the associated statistics were calculated online from the 10 Hz raw data

4

and stored in dataloggers (Model CR5000, Campbell Scientific Inc.). Other measurements such as net radiation, air temperature, humidity, and precipitation were sampled every second, averaged over 30 minutes, and logged in the dataloggers (Model CR3000 for the GDK site and CR1000 for the GCK site, Campbell Scientific Inc.). More information regarding the EC and meteorological measurements can be found in Kwon et al. (2009), and Kang et al. (2009a).

5   The multi-level profile systems were installed to measure the vertical profiles of the CO_2 and H_2O concentrations at both sites and to estimate the storage flux using a closed-path IRGA (Model: LI-6262, LI-COR Inc.). The measurement heights were 0.1, 1, 4, 8 (base of the crown), 12 (middle of the crown), 18 (the canopy top), 30, and 40 m for the GDK site and 0.1, 1, 4, 12 (base of the crown), 20 (middle of the crown), 23 (the canopy top), 30, and 40 m for the GCK site. More information regarding the multi-level profile system can be found in Hong et al. (2008) and Yoo et al. (2009).

10   To improve the data quality, the collected data were examined by the quality control procedure based on the KoFlux data processing protocol (Hong et al., 2009; Kang et al., 2014). This procedure includes a sector-wise planar fit rotation (PFR; Wilczak et al., 2001; Yuan et al., 2007; Yuan et al., 2011), the WPL (Webb-Pearman-Leuning) correction (Webb et al., 1980), a storage term calculation (Papale et al., 2006~~; see Appendix A for more details regarding the storage term calculation~~), spike detection (Papale et al., 2006), gap-filling (marginal distribution sampling method; Reichstein et al., 2005), and nighttime CO_2 flux correction (van Gorsel et al., 2009; Kang et al., 2016). The details of the gap-filling and partitioning methods are described in the next chapters.

2.3 Gap-filling and partitioning methods for the H_2O flux

2.3.1 Marginal distribution sampling (MDS) method

The missing H_2O flux (i.e., evapotranspiration, ET) data were gap-filled using the marginal distribution sampling (MDS)
20   method (Reichstein et al., 2005; Hong et al., 2009). This method calculates a median of ET under similar meteorological conditions within a time window of 14 days and replaces the missing values with the median. The intervals of the similar meteorological conditions were 50 W m^{-2} for the downward shortwave radiation (R_{sdn}), 2.5°C for the air temperature (T_a), and 5.0 hPa for the vapor pressure deficit (VPD). If similar meteorological conditions were unavailable within the time window, its interval increased in increments of 7 days before and after the missing data point (i.e., 14 days of window size)
25   until it reached 56 days (i.e., before and after 7 days → 14 days → 21 days → 28 days). When the missing ET values could not be filled in a time window less than 56 days, R_{sdn} was exclusively used following the same approach (i.e., calculating a median of ET under similar R_{sdn} conditions within a time window). This gap-filling method is used for not only the H_2O flux but also the sensible heat and daytime CO_2 fluxes.

2.3.2 Modeling of wet canopy evaporation

For estimating the wet canopy evaporation (E_{WC}), a simplified version of the Rutter sparse model (Valente et al., 1997) included in the VIC LSM (Variable Infiltration Capacity Land Surface Model, Liang et al., 1994) was used in the KoFlux data processing program. The E_{WC} is estimated as follows:

$$E_{WC\_Mod} = \sigma_f E_p \left(\frac{W_c}{S} \right)^n \left(\frac{r_a}{r_a + r_0} \right)$$

5   (1)

where E_{WC_Mod} is the modeled E_{WC}, σ_f is the vegetation fraction (i.e., 1–gap fraction); and E_p is the potential evaporation

$$E_p = \frac{\varepsilon A + \rho c_p \cdot \text{VPD} \cdot g_a / \gamma}{\lambda(\varepsilon + 1)}$$

(where ε is the dimensionless ratio of the slope of the saturation vapor pressure curve to the psychrometric constant γ, A is the available energy, ρ is the density of air, c_p is the specific heat of air, g_a is the aerodynamic conductance ($= 1/ r_a$), λ is the latent heat of vaporization); r_a is the aerodynamic resistance to heat and water

10   vapor transport; S is the canopy storage capacity; and r_0 is the architectural resistance. The term, ($r_a / (r_a + r_0)$), is added to consider the variation of the gradient of specific humidity between the leaves and the overlying air in the canopy layer. W_c is the intercepted canopy water, and the exponent n is an empirical coefficient.

W_c is estimated as:

$$\frac{\partial W_c}{\partial t} = \sigma_f P - D - E_{WC\_Mod}$$

(2)

15   where P is the input total rainfall and D is the drip. When $W_c > 0$, the canopies are wet. When $W_c > S$, the drip starts ($D > 0$). There are many inputs (i.e., E_p and P) and parameters (i.e., σ_f, S, n, r_a, and r_0) for estimating the E_{WC} and W_c. E_p, P, and r_a ($= r_{am} + r_b$ where r_{am} and r_b are the aerodynamic resistance of momentum transfer and the excess resistance; $r_{am} = \overline{U} / u_*^2$ where $\overline{U}$ is the wind speed, u^* is the friction velocity; $r_b \approx \dfrac{4.63}{u_*}$; Thom, 1972; Kim and Verma, 1990; Kang et al., 2009a)

can be obtained/estimated from the flux tower measurement. The parameters can be divided into constant parameters (i.e., n

20   and r_0) and seasonally varied parameters (i.e., σ_f and S). The default values (before optimization) of n and r_0 are 2/3 and 2 s m^{-1}, respectively. σ_f ($= 1 - $ gap fraction) and S are functions of LAI (leaf area index): (1) the gap fraction is estimated by exp($-k \times$ LAI), where k varies from 0.3 to 1.5, depending on the species and canopy structure (Jones, 2013, $k = 0.75$ and 0.485 for the GDK and GCK, respectively; (2) S is estimated by $K_L \times$ LAI, where K_L varies from 0.1 to 0.3 (default value of $K_L = 0.2$, see Appendix AB for more details). σ_f and LAI can be obtained from a plant canopy analyzer or digital

25   photography (e.g., Macfarlane et al., 2007, Hwang et al., 2016). If actual measurement is not available, MODIS (moderate-resolution imaging spectroradiometer) LAI can be used alternatively. In this study, σ_f (actually k) and LAI were estimated using a plant canopy analyzer (Model LAI-2000; Li-Cor Inc.).

The generalization of the model can be augmented by providing the parameter optimization procedure using available flux data under wet canopy condition. We argue that this is better than the validation using other datasets because the parameters may be site-specific (i.e., more validation does not fully guarantee the proposed model works properly everywhere). After optimizing the parameters (i.e., K_L, n, and r_0), the parameters slightly changed from the default values (see Appendix BC for more details). Since the model results from before and after the parameter optimization were not statistically different in the error assessment, we still used the default values in a conservative way.

This method only considers the E_{WC} from the canopy by neglecting the E_{WC} from the trunk and stem. Besides, the interception of snow is not considered because the small amount of intercepted snowfall evaporates when the eddy covariance systems function improperly, and its melting and sublimation processes are much more complex than intercepted rainfall. To distinguish snowfall from total precipitation, the empirical discriminants in Matsuo et al. (1981) were used. This method uses air temperature and humidity near the ground surface to separate snow from rainfall because when it snows, air is not saturated and the near ground air temperature is lower than that under rainy condition. The result from this method should be scrutinized by comparing it with other precipitation data, which are measured at a weather station near the site.

2.3.3 Gap-filling and partitioning technique for evapotranspiration: model-stats hybrid method

The currently used MDS is expected to under- and over-estimate ET under wet and dry canopy conditions, respectively due to the gap-filling without the consideration of canopy wetness (because the evaporative fraction is proportional to canopy wetness). Therefore, the gap-filling technique for ET proposed by Kang et al. (2012) was used: (1) to identify the canopy wetness, the intercepted canopy water (W_c, see Eq. 1) was calculated using the simplified Rutter sparse model; (2) all the missing gaps were filled by the MDS using the data under dry canopy conditions only (i.e., when $W_c = 0$), which corresponds to the ET under dry canopy condition (ET_{dry}); (3) under wet canopy conditions (i.e., when $W_c > 0$), the gap-filled data were replaced with the sum of the E_{WC} estimated by the simplified Rutter sparse model (i.e., E_{WC_Mod}) and the ET_{dry} multiplied by $1-(W_c/S)^n$ (i.e., the contribution from transpiration) (see Eqs. 1 and 2).

Such a gap-filled ET was partitioned into the transpiration (T or ET from the dry canopy, which approaches the actual transpiration under a dense and closed canopy condition) and E_{WC} as follows. In case of that the data was missing, the T was estimated as $(1-(W_c/S)^n)\,ET_{dry}$, while the E_{WC} was estimated as E_{WC_Mod}. In case of that the data was not missing (i.e., ET_{Obs}), the partitioning procedure divided into two parts. If the signs of ET_{Obs}, ET_{dry}, and E_{WC_Mod} were the same, the T was estimated by multiplying ET_{Obs} and the ratios of $(1-(W_c/S)^n)\,ET_{dry}$ to the sum of $(1-(W_c/S)^n)\,ET_{dry}$ and E_{WC_Mod} (i.e., the estimated transpired-fraction of ET), while the E_{WC} was estimated by multiplying ET_{Obs} and the ratios of E_{WC_Mod} to the sum of $(1-(W_c/S)^n)\,ET_{dry}$ and E_{WC_Mod} (i.e., the estimated evaporated-fraction of ET). If the signs of ET_{Obs}, ET_{dry}, and E_{WC_Mod} were not the same, the T were estimated by $(1-(W_c/S)^n)\,ET_{dry}$, while the E_{WC} was estimated by subtracting $(1-(W_c/S)^n)\,ET_{dry}$ (i.e., the estimated T) from ET_{Obs}. The procedure regarding the MSH is described in Fig. 1.

[Figure 1 here]

2.4 Correction and partitioning methods for the CO_2 flux

2.4.1 General nighttime CO_2 flux correction methods

The KoFlux protocol includes three different nighttime corrections methods: the friction velocity (u^*) filtering method (FVF), the light response curve method (LRC), and the modified van Gorsel method (VGF) (van Gorsel et al., 2009; Kang et al., 2014 and 2017). These three filtering methods each have their own way of selecting good quality CO_2 flux data. The site-specific settings of the individual methods were as follows: 1) the lower u^* threshold for the FVF was 0.3 m s^{-1} for both the GDK and GCK sites. (We checked the dependency of nighttime CO_2 flux on friction velocity during the growing and dormant seasons (not shown here). 0.3 m s^{-1} of u^* threshold can be determined during the growing season, while it is hard to clearly decide a threshold during the dormant season for the both sites. But, the threshold during the dormant season would be smaller than 0.3 m s^{-1}. Thus, we applied the constant threshold of 0.3 m s^{-1} for the sites (conservative approach similarly to Reichstein et al., 2005)), 2) the Michaelis Menten type light response curve ($$ NEE = R_{LRCd} - (\alpha Q_t A_{max} / \alpha Q_t + A_{max}) $$, where R_{LRCd} is the estimated mean daytime RE, α is the apparent quantum yield, A_{max} is the canopy scale photosynthetic capacity, and Q_t is the total incident shortwave radiation above the canopy; van Gorsel et al., 2009) was used for the LRC, and 3) the peak of the F_{CO2_Obs} that occurred approximately at sunset (R_{max}) was directly used for the modified VGF after calculating the median diurnal variation of the CO_2 flux for a certain period (Kang et al., 2014 and 2017).The modified VGF produces a similar result to that from the original VGF for the sites (see Appendix D for more details regarding the modified VGF). We applied a 30-day moving window to obtain the daily R_{LRCd} and R_{max}.

The selected RE data from each filtering method were processed as follows. First, we estimated the parameters in the RE equation (Lloyd Taylor equation, $$ RE = R_{ref} \exp(E_0(1/T_{ref} - T_0) - 1/(T_a - T_0))) $$, where R_{ref} is the reference RE, T_{ref} is the reference temperature (= 10°C), E_0 is the activation energy parameter (°C^{-1}), T_0 is -46.02°C and T_a is the air temperature (°C), using the selected observed RE (Lloyd and Taylor, 1994). Second, we replaced the bad (or missing) data with the calculated data using the air temperature and the RE function with the estimated parameters. We estimated R_{ref} using a 30-day moving window which was shifted every 5 days to consider the variations of a RE controlled by soil moisture and phenology, which is not considered in the Lloyd Taylor equation. The E_0 is constant for each site year, which is estimated using the generic algorithm proposed by Reichstein et al. (2005) that derives a short term temperature sensitivity (see Reichstein et al., 2005; Hong et al., 2009 for more details). Each method was independent each other. In cases of the LRC method and the modified VGF, the nighttime CO_2 fluxes were filtered out when the observed nighttime CO_2 fluxes were underestimated out of the 95% confidence interval of the RE model (i.e., Lloyd and Taylor equation). GPP was calculated by subtracting NEE from RE.

2.4.2 A modification of the moving point test method (MPT)

The objective of the moving point test (MPT) method is to determine the intermediate range of u^* where the nighttime CO_2 fluxes are independent of u^* (Gu et al., 2005). The method searches for lower and higher u^*-thresholds, which are found by statistically testing (i.e., t test) a group of points with consecutive u^*-values in a narrow moving window against a reference sample. The original method excludes night data when the median u^* were lower than the lower u^* threshold, to avoid an underestimation of the CO_2 flux due to drainage flow. However, this consideration is inappropriate for hilly terrain sites that are usually affected by drainage flow (e.g., the study sites, GDK and GCK), resulting in that the CO_2 fluxes were close to 0 and/or much smaller than the true values during most of nighttime except near sunset.

Thus, we modified the original MPT method to apply it to hilly terrain sites by: (1) splitting it into the two time windows, i.e., the time window near sunset (when a drainage has not yet (completely) manifested. It had been directly/indirectly proven using the bulk Richardson number, the CO_2 concentration profile, the CO_2 flux measured by chamber method (van Gorsel et al., 2007, 2008) and the information flow between the uphill and downhill (Kang et al., 2017) in the previous studies.) and the time window after the former, (2) applying the MPT method to each time window, (3) comparing the results between the two time windows and determining the existence of CO_2 drainage (i.e., the averages of the normalized nighttime CO_2 fluxes for the two time windows were significantly different), and (4) excluding all the data in the second time window if the CO_2 drainage is commonly generated (i.e., showing the significant difference between the averages) and then applying the FVF method for the both time windows using the u^* thresholds determined in the previous steps.

The best feature of the modified MPT is that the time is split into the two time windows based on van Gorsel et al. (2009): (1) for calculating the median diurnal variation of the CO_2 flux and identifying whether the peak of NEE occurred approximately at sunset; (2) splitting the time windows, i.e., the first window one and two hours before and after the time of peak occurrence, respectively; and the second window of the time after the first time window.

The assumption of this method is that the biological and meteoroidal conditions that can affect the RE are not significantly different between the two time windows. For the study sites, the mountain wind rose consistently at night, and we did not find any driver which makes a difference between the averages of RE in the two time windows except ecosystem temperature. Thus, we compared the averages after normalizing the flux measurements using the temperature response function (i.e., Lloyd and Taylor equation) as same as the original MPT method proposed by Gu et al. (2005).

For applying the MPT method, there were two criteria, i.e., the significance level in the t test (α) and the size (i.e., the number of data) of the moving sample (n). According to Gu et al. (2005), the α is 0.1, and the n is 25. The MPT method was applied for every three months. The details regarding the (modified) MPT are described in the flow charts (Fig. 2) and Gu et al. (2005).

[Figure 2 here]

3 Results

~~3.1 Gap-filling and partitioning results for the H$_2$O flux~~

3.1.~~1~~ Validation of the MSH

First, we evaluated the latent heat flux under (mostly) wet canopy conditions (λET_{WC}, i.e., λET when $W_c/S > 2/3$) from the

5 model-stats hybrid (MSH) method (λET_{WC_MSH}) against the observed λET_{WC} (λET_{WC_Obs}) at both sites from 2008 to 2010 (Fig. 2~~3~~). Since the λET_{WC} occurs in during and following rain events, open-path EC system can measure the λET_{WC} when the instrument dries out faster than the canopy. Most of the points are near a one-to-one line. The data scattered away from the one-to-one line are characterized by large aerodynamic conductance (e.g., >100 mm s^{-1}) and/or large VPD (e.g., >10 hPa).

10 [Figure 2~~3~~ here]

Table 1 shows the statistical parameters for the error assessment (i.e., MBE, MAE, RMSE, d, slope, and r^2; see Appendix D~~E~~ for more details about the error assessment). The slopes from the linear regression analysis are 0.97±0.15 and 0.89±0.07 with 0.69±0.06 and 0.81±0.02 of r^2 for the GDK and GCK sites, respectively. The d values for the sites were close to 1

15 (0.91±0.01 for the GDK and 0.95±0.01 for the GCK). Compared to the previous research (i.e., Kang et al., 2012), the results from the MSH were closer to the observation due to the consideration of ET from the dry canopy. One of the leading causes of the error in λET_{WC_MSH} was identified as the discrepancy between the time when the rain occurred, and the tipping bucket was tipped. The results from the further evaluation of the MSH using a closed-path EC system were similar to those using the open-path EC system (see the Appendix C). To validate only E_{WC}, cross-validation using the other models (e.g., Gash

20 sparse analytical model, Gash et al., 1995) can be attempted (e.g., Kang et al., 2012). Overall, the results from the linear regression analysis of λET_{WC_MSH} and λET_{WC_Obs} show that MSH can provide λET_{WC} reasonably well for the sites.

[Table 1 here]

25 ### 3.1.~~1.~~2 Comparison between the MDS and the MSH

To evaluate the superiority of the MSH, we filled up the missing λET_{WC} data by using the MDS (λET_{WC_MDS}) and the MSH (λET_{WC_MSH}). The underestimation of the λET_{WC_MDS} had been shown by the comparison with the sum of energy flux components except for latent heat flux (= net radiation + sensible heat flux + storage flux) in our previous study (Kang et al. 2012). The λE_{WC_mod} displayed the mirrored patterns of the sum of the other energy budget components, while the λET_{WC_MDS}

30 were very small (mainly due to the low radiation during the rainy days). Thus, we expected that the MDS underestimates the ET since it cannot explicitly consider the key processes of wet canopy evaporation (i.e., the effects of aerodynamic

conductance (g_a) change and sensible heat advection, see Kang et al., 2012 for more detailed explanation). Actually, the average annual MBEs from 2008 to 2010 were -18±6 W m^{-2} for the GDK site and -15±5 W m^{-2} for the GCK site, respectively. It also should be noted that the λET_{WC_MSH} varied while λET_{WC_MDS} were nearly constant occasionally, because (1) the λET_{WC_Obs} rarely existed close to the missing data and (2) the MDS did not consider the effect of g_a (not shown here).

5   Figure 34 shows the monthly ETs gap-filled by the MDS and MSH methods for the GDK and GCK sites. First, the annual ETs from the MSH method were 16 ~ 41 mm year^{-1}, which is significantly larger than those from the MDS method, while the random uncertainties in gap-filled annual ETs were approximately 5 mm year^{-1} for the both sites (quantified according to Finkelstein and Sims, 2001, and Richardson and Hollinger, 2007). The significant difference was identified in June, July, August, and September when it was intensive rainfall. The biggest difference is shown in 2010 with more frequent and larger

10   rainfall (for the GDK, the number of rainy days is 86, 82, and 103 days and the total amount of rainfall is 1,407, 1,323, and 1,652 mm in 2008, 2009, and 2010, respectively. Such characteristics are similar to those for the GCK). In addition to taking the missing E_{WC} from the MDS into account, the other advantage of the MSH method is that the observed in ET and by eddy covariance system can be partitioned into transpiration (T) and E_{WC} without any additional measurement. However, it can be applied to a dense canopy only, where soil evaporation is negligible. Otherwise, (e.g., before leaf unfolding and after leaf

15   fall), the T includes the error of the soil evaporation (E_S). Thus, there is more separating the E_{WC} than partitioning the ET. The annual E_{WC} ranged from 53 mm to 82 mm for the GDK and 78 mm to 112 mm for the GCK, which occupies 14 ~ 23% and 14 ~ 19% of the annual ET, respectively.

     For quantifying the E_S, the supplementary eddy covariance (EC) systems were operated at the floors of the GDK and GCK sites (Kang et al. 2009b). The annual understory ET (~ E_S) from 1 June 2008 to 31 May 2009 was 59 mm for the GDK and

20   43 mm for the GCK, which occupied 16% and 8% of the annual ET, respectively. The decoupling factor (Ω, McNaughton and Jarvis, 1983) at the forest floor was ~ 0.15 for the both sites approximately, which indicates that the E_S was controlled primarily by the VPD and surface conductance (g_s) rather than R_{sdn}. This factor also suggests that separating E_S from ET using the exponential radiation extinction model to estimate the R_{sdn} at the forest floor and the relationship between the estimated R_{sdn} and the ET when the canopy is inactive (Stoy et al., 2006) can be problematic for the sites. Considering that

25   the accurate estimation of g_s is challenging, a supplementary measurement (e.g., low-level EC, lysimeter, sap-flow measurement, and isotope) is a better approach for estimating E_S. Using the E_S measured by the low-level EC, the annual T can be estimated at 265 mm (70% of ET) for the GDK and 448 mm (78% of ET) for the GCK, while the E_{WC} estimated as 55 mm (15% of ET) and 82 mm (14% of ET), respectively (Fig. 34).

30   [Figure 34 here]

11

3.2 Correcting and partitioning results for the CO_2 flux

3.2.1 Validation of the modified MPT

Figure 5 shows a part of the results from the modified moving point test (MPT) method for the GCK in 2008. During DOY 91-181, the averages of the normalized nighttime CO_2 fluxes (after the u^* filtering) for the two time windows (i.e., the time window near sunset (when drainage has not yet (completely) manifested (1st time window) and the time window after the former (2nd time window)) was statistically the same. The result suggests that there is no drainage and/or the drainage effect is negligible. Meanwhile, during DOY 1-90, those are significantly different, suggesting that the observation for the 2nd time window cannot represent the actual ecosystem respiration due to the drainage. Many points for the 2nd time window are near 0 although the air temperature is higher than 0 °C (Fig. 5(b)). The results from the modified MPT are summarized in Table 2. It is hard to find a certain characteristic of the drainage effect, implying that it is a consequence complexly influenced by micrometeorology, phenology, and data availability. Such results require careful examinations from micrometeorological and ecological perspectives using the other independent observations because the modified MPT is a kind of empirical correction.

[Figure 5 here]

[Table 2 here]

To validate the results from the modified MPT, we compared the results to those from a previous study (Kang et al. 2017). They developed the site-specific quality control filter to exclude data strongly affected by CO_2 advection, which identifies the observations when a high information flow toward the bottom of the slope exists in the dynamical process network based on the observed multi-level CO_2 concentrations at the GDK and GCK sites. The filter discards the data (1) when the CO_2 drainage is fully generated as the mountain wind prevails (i.e., 21:00 to 9:00, 8:00, and 7:30 for the dormant, transition, and growing seasons, respectively), (2) when u^* is lower than the threshold (0.3 m s^{-1}) while the drainage flow is under strong development (from 17:00 to 21:00), and (3) until the accumulated CO_2 completely dissipates for the downhill (GCK) site (i.e., before noon). Figure 6 shows the (averaged) annual CO_2 budget from the three general nighttime correction methods (see the Chapter 2.4.1) after applying the filter (Currently (without other independent measurements such as chamber method), it was the most reliable result) and that from the modified MPT method for the sites. Almost all the results agree with each other within the margin of error, indicating the validity of the modified MPT method. Additionally, we compared the annual net ecosystem production (NEP, = net primary production (NPP) – heterotrophic respiration) with the diameter at breast height (DBH) increment (which is directly related to the NPP) for the GCK site with the single dominant species (i.e., *Abies holophylla*). The both show similar interannual variability, which also can support the reasonability of the method (Fig. 7, even though there was a limitation because the heterotrophic respiration was not considered).

[Figure 6 here]

12

4 Applications

In this chapter, we illustrate the advantages of the proposed technique~~s. Mostly, t~~The benefits are caused by the gap-filling and partitioning of the H$_2$O flux because the model-stats hybrid (MSH) method can take the E_{WC} into account properly and separate them from ET, which has not yet been previously possible. ~~On the other hand, the modified moving point test (MPT) method has an improved applicability because it can be applied regardless of topography.~~ We hope the following chapters draw attention to the ET partitioning.

4.1 Wavelet coherence analysis between ET and the rainfall

To evaluate the effect of new gap-filling, we conducted the wavelet coherence analysis between ET and rainfall for the GDK site (Fig. ~~4~~8, see Hong et al. (2010) and Grinsted et al. (2004) for more details regarding the wavelet coherence analysis). From one- to the third month period, which was the three-month period in the monsoon season (i.e., the intensive rainy period), high correlation (i.e., red color area) was observed between ET and rainfall in 2006, 2007, 2008, and 2009. In 2007, the rainfall amount was 200 mm lower than the average level during the study period. However, the rainfall duration was the longest, and the intensity was the lowest. In 2006, 2008, and 2009, the arrow on the high correlation area pointed left. It means a negative correlation between the two variables, reflecting that the decrease in T caused by the diminishment of R_{sdn} during the intensive rainy period. In contrast, the arrow pointed right in 2007, indicating a positive correlation. The magnitude of enhanced E_{WC} was greater than that of decreased T at that time and frequency in 2007. Such a positive correlation between ET and rainfall with one- to three-month cycle in 2007 was not reported in the previous study of Hong et al. (2010) which showed a negative correlation in 2006, 2007 and 2008 at that time and frequency. This can be attributed to the improvement in ET data made by the new gap-filling method (i.e., recovering the missing E_{WC} in the general gap-filling method). During the monsoon season, the E_{WC} compensates (a portion of) the decreased T, and it can occasionally be balanced (e.g., in 2010).

There are some circumstantial evidences which support that the proposed method is more appropriate for taking E_{WC} into account than the conventional method: (1) the ratio of the runoff and the precipitation (adapted from Choi et al. 2011) in 2007 was the lowest (0.60 in 2007, 0.69±0.06 in the other years, i.e., the ratio of the ET to the precipitation can be the highest in 2007), while the $\underline{R_{sdn}}$ (main controlling factor of T) was the lowest (4.52 GJ m^{-2} in 2007, 4.77±0.08 GJ m^{-2} in the other years) due to the longest rainfall duration, (2) the interannual variabilities of the estimated catchment scale annual ET (i.e., precipitation – runoff) and ET from the MDS method occurred in opposite directions (similarly to T from the MSH method).

[Figure ~~4~~8 here]

4.2 Water use efficiency at the ecosystem-level and the canopy-level

Water use efficiency (WUE) can be defined in various forms such as A_n/g_{st} (intrinsic WUE; A_n: net assimilation; g_{st}: stomatal conductance; A_n=NPP), A_n/T (instantaneous WUE), $A_n(1-\Phi_c)/[T(1+\Phi_w)]$ (integrated WUE; Φ_c: fraction of assimilated carbon lost in respiration; Φ_w: fraction of total water loss from non-photosynthetic parts of the plant or through open stomata at night), the GPP/T (canopy-level WUE), NPP/ET (stand-level WUE), and GPP/ET (ecosystem-level WUE) (Seibt et al., 2008; Ito and Inatomi, 2012; Ponton et al., 2006), because the spatiotemporal scale and measurement method are research-specific. Based on the original definition of WUE (i.e., the ratio of CO_2 flux to H_2O flux), we re-defined the annual ecosystem-level WUE (WUE_{Eco}) and the annual canopy-level WUE (WUE_{Canopy}) as $\Sigma NEP/\Sigma ET$ and $\Sigma NPP/\Sigma T$, respectively. For estimating ΣNPP and ΣT simply, we used 0.45 of the ratio of the NPP to GPP for the both sites (Waring et al., 1998), and 0.156 and 0.075 of the ratios of E_S to ET for the GDK and GCK, respectively (Kang et al., 2009b). From 2006 to 2010, WUE_{Eco} (WUE_{Canopy}) ranged from -0.16 (2.17) to 0.32 (2.59) g C·(kg H_2O)$^{-1}$ for the GDK site and from 0.20 (1.93) to 0.38 (2.16) g C·(kg H_2O)$^{-1}$ for the GCK site (Table 2~~3~~). Considering the increasing trend of NEE and GPP for the GCK site, it can be identified that the interannual variabilities of WUE_{Eco} and WUE_{Canopy} occurred in opposite directions for the both sites. It was primarily caused by that E_{WC} were enhanced in 2007 and 2010 due to the weakest rainfall intensity and the largest rainfall amount, respectively. Overall, such partitioning of the total ET into E_{WC}, T, and E_S enables us to understand better how ET responses to environmental changes and the how water cycle is connected to the carbon cycle in a forest ecosystem.

[Table 2~~3~~ here]

5 Conclusions

There is a ~~common characteristic between~~special feature of the new~~two~~ technique~~s~~ proposed in this study for gap-filling and partitioning of H_2O ~~and CO_2~~ eddy fluxes: two existing methods were merged into a new method. The marginal distribution sampling (MDS) method and the simplified Rutter spars model have merged into the model-stats hybrid (MSH) method ~~and the u^* filtering (i.e., moving point test method, MPT) and van Gorsel methods were merged into the modified MPT~~. Such a strategy strengthens the strength and makes up for the weakness of the original methods. ~~Especially, the modified MPT for nighttime CO_2 flux correction substantially improves its applicability, expecting that it will contribute to the standardization of eddy covariance data processing.~~ In this context, such attempt will and must continue. The MSH method can be applied to tropical forests because tropical forests also share three properties of temperate forests (i.e., extensive, dense, and tall). However, applying the methods to grasslands may need further validation.

14

Acknowledgments

References

Aboal, J. R., Jiménez, M. S., Morales, D., and Hernández, J. M.: Rainfall interception in laurel forest in the Canary Islands, Agric. For. Meteorol., 97, 73-86, 1999.

Aubinet, M., Chermanne, B., Vandenhaute, M., Longdoz, B., Yernaux, M., and Laitat, E.: Long term carbon dioxide exchange above a mixed forest in the Belgian Ardennes, Agric. For. Meteorol., 108, 293-315, 2001.

Baldocchi, D. D., Hicks, B. B., and Meyers, T. P.: Measuring biosphere-atmosphere exchanges of biologically related gases with micrometeorological methods, Ecology, 69, 1331-1340, 1988.

Carlyle-Moses, D. E., and Price, A. G.: Modelling canopy interception loss from a Madrean pine-oak stand, northeastern Mexico, Hydrol. Process., 21, 2572-2580, 2007.

Choi, H. T.: Effect of forest growth and thinning on the long-term water balance in a coniferous forest, Korean J. Agric. For. Meteorol., 13, 157-164, 2011 (in Korean with English abstract).

Crockford, R. H., and Richardson, D. P.: Partitioning of rainfall into throughfall, stemflow and interception effect of forest type, ground cover and climate, Hydrol. Process., 14, 2903-2920, 2000.

Daikoku, K., Hattori, S., Deguchi, A., Aoki, Y., Miyashita, M., Matsumoto, K., Akiyama, J., Iida, S., Toba, T., and Fujita, Y.: Influence of evaporation from the forest floor on evapotranspiration from the dry canopy, Hydrol. Process., 22, 4083-4096, 2008.

Deardorff, J.W.: Efficient prediction of ground surface temperature and moisture,w ith inclusiono f a layer of vegetation, J, . Geophy. Res., 83, 1889-1903, 1978.

Deguchi, A., Hattori, S., and Park, H. T.: The influence of seasonal changes in canopy structure on interception loss: Application of the revised Gash model, J. Hydrol., 318, 80-102, 2006.

Dickinson,R .E.: Modelling evapotranspiratio for three-dimensional global climate models, in Climate Processes and Climate Sensitivity, Geophys. Monogr. Set., vol. 29, edited by J.E. Hansen and T. Takahashi, pp. 58-72, AGU, Washington, D.C., 1984.

Dunkerley, D. L.: Evaporation of impact water droplets in interception processes: Historical precedence of the hypothesis and a brief literature overview, J. Hydrol., 376, 599-604, 2009.

Falge, E., Baldocchi, D., Olson, R., Anthoni, P., Aubinet, M., Bernhofer, C., Burba, G., Ceulemans, R., Clement, R., Dolman, H., Granier, A., Gross, P., Grunwald, T., Hollinger, D., Jensen, N. O., Katul, G., Keronen, P., Kowalski, A., Ta Lai,

~~C., Law, B. E., Meyers, T., Moncrieff, J., Moors, E., William Munger, J., Pilegaard, K., Rannik, U., Rebmann, C., Suyker, A., Tenhunen, J., Tu, K., Verma, S., Vesala, T., Wilson, K., and Wofsy, S.: Gap filling strategies for long term energy flux data sets, Agric. For. Meteorol., 107, 71-77, 2001.~~

Fratini, G., Ibrom, A., Arriga, N., Burba, G., and Papale, D.: Relative humidity effects on water vapour fluxes measured with closed-path eddy-covariance systems with short sampling lines, Agric. For. Meteorol., 165, 53-63, 2012.

Gash, J. H., Lloyd, C. R., and Lachaud, G.: Estimating sparse forest rainfall interception with an analytical model, J. Hydrol., 170, 79-86, 1995.

Goodrich, J. P., Oechel, W. C., Gioli, B., Moreaux, V., Murphy, P. C., Burba, G., and Zona, D.: Impact of different eddy covariance sensors, site set-up, and maintenance on the annual balance of CO_2 and CH_4 in the harsh Arctic environment. Agric. For. Meteorol., 228, 239-251, 2016.

Grinsted, A., Moore, J. C., and Jevrejeva, S.: Application of the cross wavelet transform and wavelet coherence to geophysical time series, Nonlinear Process Geophys., 11, 561-566, 2004.

~~Gu, L., Falge, E. M., Boden, T., Baldocchi, D. D., Black, T., Saleska, S. R., Suni, T., Verma, S. B., Vesala, T., and Wofsy, S. C.: Objective threshold determination for nighttime eddy flux filtering, Agric. For. Meteorol., 128, 179-197, 2005.~~

Hong, J., and Kim, J.: Impact of the Asian monsoon climate on ecosystem carbon and water exchanges: a wavelet analysis and its ecosystem modeling implications, Global Change Biol., 17, 1900-1916, 2011.

Hong, J., Kim, J., Lee, D., and Lim, J. H.: Estimation of the storage and advection effects on H_2O and CO_2 exchanges in a hilly KoFlux forest catchment, Water Resour. Res., 44, 2008.

Hong, J.., Kwon, H.-J., Lim, J.-H., Byun, Y.-H., Lee, J.-H., and Kim, J.: Standardization of KoFlux eddy-covariance data processing, Korean J. Agric. For. Meteorol., 11, 19-26, 2009 (in Korean with English abstract).

Hong, J., Lee, D., Kim, J: Lessons from FIFE (First ISLSCP Field Experiment) inscaling issues of surface fluxes at Gwangneung supersite. Korean J. Agric. For. Meteorol. 7, 4–14, 2005 (in Korean with English abstract).

Hu, Z., Yu, G., Zhou, Y., Sun, X., Li, Y., Shi, P., Wang, Y., Song, X., Zheng, Z., and Zhang, L.: Partitioning of evapotranspiration and its controls in four grassland ecosystems: Application of a two-source model, Agric. For. Meteorol., 149, 1410-1420, 2009.

Hwang, Y., Ryu, Y., Kimm, H., Jiang, C., Lang, M., Macfarlane, C., and Sonnentag, O.: Correction for light scattering combined with sub-pixel classification improves estimation of gap fraction from digital cover photography, Agric. For. Meteorol., 222, 32-44, 2016.

Ibrom, A., Dellwik, E., Flyvbjerg, H., Jensen, N. O., and Pilegaard, K.: Strong low-pass filtering effects on water vapour flux measurements with closed-path eddy correlation systems, Agric. For. Meteorol., 147, 140-156, 2007.

Ito, A., and Inatomi, M.: Water-use efficiency of the terrestrial biosphere: a model analysis focusing on interactions between the global carbon and water cycles, J. Hydrometeorol., 13, 681-694, 2012.

Jones, H. G.: Plants and microclimate: a quantitative approach to environmental plant physiology, Cambridge university press, 9-46, 2013.

Kang, M., Kim, J., Kim, H.-S., Thakuri, B. M., and Chun, J.-H.: On the nighttime correction of CO_2 flux measured by eddy covariance over temperate forests in complex terrain, Korean Journal of Agric. For. Meteorol., 16, 233-245, 2014 (in Korean with English abstract).

Kang, M., Kwon, H., Cheon, J. H., and Kim, J.: On estimating wet canopy evaporation from deciduous and coniferous forests in the Asian monsoon climate, J. Hydrometeorol., 13, 950-965, 2012.

Kang, M., Park, S., Kwon, H., Choi, H. T., Choi, Y. J., and Kim, J.: Evapotranspiration from a deciduous forest in a complex terrain and a heterogeneous farmland under monsoon climate, Asia-Pac. J. Atmos. Sci., 45, 175-191, 2009a.

Kang, M., Ruddell, B. L., Cho, C., Chun, J., and Kim, J.: Identifying CO_2 advection on a hill slope using information flow, Agric. For. Meteorol., 232, 265-278, 2017.

Kang, M., Kwon, H., Lim, J.-H., and Kim, J.: Understory evapotranspiration measured by eddy-covariance in Gwangneung deciduous and coniferous forests, Korean J. Agric. For. Meteorol., 11, 233-246, 2009b (in Korean with English abstract).

Kang, M., Thakuri, M. B., Kim, J., Chun, J., and Cho, C.: A modification of the moving point test method for nighttime eddy flux filtering on hilly and complex terrain, Abstract B41B-0404 presented at 2016 Fall Meeting, AGU, San Francisco, Calif., 2016.

Kim, J., Lee, D., Hong, J., Kang, S., Kim, S.-J., Moon, S.-K., Lim, J.-H., Son, Y., Lee, J., Kim, S., Woo, N., Kim, K., Lee, B., Lee, B.-L., and Kim, S.: HydroKorea and CarboKorea: cross-scale studies of ecohydrology and biogeochemistry in a heterogeneous and complex forest catchment of Korea, Ecol. Res., 21, 881-889, 2006.

Kim, J., and Verma, S. B.: Components of surface energy balance in a temperate grassland ecosystem, Bound.-Layer Meteor., 51, 401-417, 1990.

Kwon, H., Park, T.-Y., Hong, J., Lim, J.-H., and Kim, J.: Seasonality of Net Ecosystem Carbon Exchang in Two Major Plant Functional Types in Korea, Asia-Pac. J. Atmos. Sci., 45, 149-163, 2009.

Lankreijer, H., Lundberg, A., Grelle, A., Lindroth, A., and Seibert, J.: Evaporation and storage of intercepted rain analysed by comparing two models applied to a boreal forest, Agric. For. Meteorol., 98-99, 595-604, 1999.

Liang, X., Lettenmaier, D. P., Wood, E. F., and Burges, S. J.: A simple hydrologically based model of land surface water and energy fluxes for general circulation models, J. Geophys. Res. Atmos., 99, 14415-14428, 1994.

Lloyd, J., and Taylor, J.: On the temperature dependence of soil respiration, Funct. Ecol., 315-323, 1994.

Macfarlane, C., Hoffman, M., Eamus, D., Kerp, N., Higginson, S., McMurtrie, R., and Adams, M.: Estimation of leaf area index in eucalypt forest using digital photography, Agric. For. Meteorol., 143, 176-188, 2007.

Marin, C. T., Bouten, W., and Sevink, J.: Gross rainfall and its partitioning into throughfall, stemflow and evaporation of intercepted water in four forest ecosystems in western Amazonia, J. Hydrol., 237, 40-57, 2000.

Matsuo, T., Sasyo, Y., and Sato, Y.: Relationship between types of precipitation on the ground and surface meteorological elements, J. Meteorol. Soc. Japan, Ser. II, 59, 462-476, 1981.

Moon, S.-K., Park, S.-H., Hong, J., and Kim, J.: Spatial characteristics of Gwangneung forest site based on high resolution satellite images and DEM, Korean J. Agric. For. Meteorol., 7, 115-123, 2005 (in Korean with English abstract).

Murakami, S.: Application of three canopy interception models to a young stand of Japanese cypress and interpretation in terms of interception mechanism, J. Hydrol., 342, 305-319, 2007.

5   Papale, D.: Data gap filling. In Eddy Covariance (pp. 159-172). Springer Netherlands, 2012.

Papale, D., Reichstein, M., Aubinet, M., Canfora, E., Bernhofer, C., Kutsch, W., Longdoz, B., Rambal, S., Valentini, R., and Vesala, T.: Towards a standardized processing of Net Ecosystem Exchange measured with eddy covariance technique: algorithms and uncertainty estimation, Biogeosciences, 3, 571-583, 2006.

Papale, D., and Valentini, R.: A new assessment of European forests carbon exchanges by eddy fluxes and artificial neural network spatialization, Global Change Biol., 9, 525-535, 2003.

10

Perrier, A.: Etude physique de l'évapotranspiration dans les conditions naturelles. III. Evapotranspiration réelle et potentielle des couverts végétaux. In Annales agronomiques, 1975.

Ponton, S., Flanagan, L. B., Alstad, K. P., Johnson, B. G., Morgenstern, K., Kljun, N., Black, T. A., and Barr, A. G.: Comparison of ecosystem water-use efficiency among Douglas-fir forest, aspen forest and grassland using eddy covariance and carbon isotope techniques, Global Change Biol., 12, 294-310, 2006.

15

Pypker, T. G., Bond, B. J., Link, T. E., Marks, D., and Unsworth, M. H.: The importance of canopy structure in controlling the interception loss of rainfall: Examples from a young and an old-growth Douglas-fir forest, Agric. For. Meteorol., 130, 113-129, 2005.

Rana, G., Katerji, N., Mastrorilli, M., and El Moujabber, M.: Evapotranspiration and canopy resistance of grass in a Mediterranean region. Theor. Appl. Climatol., 50, 61-71, 1994.

20

Reichstein, M., Falge, E., Baldocchi, D., Papale, D., Aubinet, M., Berbigier, P., Bernhofer, C., Buchmann, N., Gilmanov, T., Granier, A., Grunwald, T., Havrankova, K., Ilvesniemi, H., Janous, D., Knohl, A., Laurila, T., Lohila, A., Loustau, D., Matteucci, G., Meyers, T., Miglietta, F., Ourcival, J.-M., Pumpanen, J., Rambal, S., Rotenberg, E., Sanz, M., Tenhunen, J., Seufert, G., Vaccari, F., Vesala, T., Yakir, D., and Valentini, R.: On the separation of net ecosystem exchange into assimilation and ecosystem respiration: review and improved algorithm, Global Change Biol., 11, 1424-1439, doi:10.1111/j.1365-2486.2005.001002.x, 2005.

25

Reichstein, M., Stoy, P. C., Desai, A. R., Lasslop, G., and Richardson, A. D.: Partitioning of net fluxes. In Eddy Covariance (pp. 263-289). Springer Netherlands, 2012.

Schellekens, J., Scatena, F. N., Bruijnzeel, L. A., and Wickel, A. J.: Modelling rainfall interception by a lowland tropical rain forest in northeastern Puerto Rico, J. Hydrol., 225, 168-184, 1999.

30

Seibt, U., Rajabi, A., Griffiths, H., and Berry, J. A.: Carbon isotopes and water use efficiency: sense and sensitivity, Oecologia, 155, 441, 2008.

18

Shi, Z., Wang, Y., Xu, L., Xiong, W., Yu, P., Gao, J., and Zhang, L.: Fraction of incident rainfall within the canopy of a pure stand of Pinus armandii with revised Gash model in the Liupan Mountains of China, J. Hydrol., 385, 44-50, 10.1016/j.jhydrol.2010.02.003, 2010.

Shuttleworth, W., Leuning, R., Black, T., Grace, J., Jarvis, P., Roberts, J., and Jones, H.: Micrometeorology of temperate and tropical forest, Phil. Trans. R. Soc. B, 324, 299-334, 1989.

Silva, I. C., and Okumura, T.: Rainfall partitioning in a mixed white oak forest with dwarf bamboo undergrowth, J. Environ. Hydrol., 4, XIII-XIV, 1996.

Šraj, M., Brilly, M., and Mikoš, M.: Rainfall interception by two deciduous Mediterranean forests of contrasting stature in Slovenia, Agric. For. Meteorol., 148, 121-134, 2008.

Stoy, P. C., Katul, G. G., Siqueira, M. B. S., Juang, J. Y., Novick, K. A., McCarthy, H. R., Oishi, A. C., Uebelherr, J. M., Kim, H. S., and Oren, R.: Separating the effects of climate and vegetation on evapotranspiration along a successional chronosequence in the southeastern US, Global Change Biol., 12, 2115-2135, 10.1111/j.1365-2486.2006.01244.x, 2006.

Thom, A. S.: Momentum, Mass, and Heat Exchange of Vegetation, Quart. J. Roy. Meteor. Soc., 98, 124–134, 1972.

Valente, F., David, J. S., and Gash, J. H. C.: Modelling interception loss for two sparse eucalypt and pine forests in central Portugal using reformulated Rutter and Gash analytical models, J. Hydrol., 190, 141-162, 1997.

Van Dijk, A. I. J. M., and Bruijnzeel, L. A.: Modelling rainfall interception by vegetation of variable density using an adapted analytical model. Part 2. Model validation for a tropical upland mixed cropping system, J. Hydrol., 247, 239-262, 2001.

van Gorsel, E., Delpierre, N., Leuning, R., Black, A., Munger, J. W., Wofsy, S., Aubinet, M., Feigenwinter, C., Beringer, J., and Bonal, D.: Estimating nocturnal ecosystem respiration from the vertical turbulent flux and change in storage of CO_2, Agric. For. Meteorol., 149, 1919-1930, 2009.

van Gorsel, E., Leuning, R., Cleugh, H. A., Keith, H., Kirschbaum, M. U., and Suni, T.: Application of an alternative method to derive reliable estimates of nighttime respiration from eddy covariance measurements in moderately complex topography, Agric. For. Meteorol., 148, 1174-1180, 2008.

Van Gorsel, E., Leuning, R., Cleugh, H. A., Keith, H., and Suni, T.: Nocturnal carbon efflux: Reconciliation of eddy covariance and chamber measurements using an alternative to the u*-threshold filtering technique, Tellus B, 59, 397-403, 2007.

Waring, R., Landsberg, J., and Williams, M.: Net primary production of forests: a constant fraction of gross primary production?, Tree physiol., 18, 129-134, 1998.

Webb, E. K., Pearman, G. I., and Leuning, R.: Correction of flux measurements for density effects due to heat and water vapour transfer, Q. J. R. Meteorol. Soc., 106, 85-100, 10.1002/qj.49710644707, 1980.

Wilczak, J., Oncley, S., and Stage, S.: Sonic Anemometer Tilt Correction Algorithms, Boundary-Layer Meteorol., 99, 127-150, 2001.

Willmott, C. J.: Some comments on the evaluation of model performance, Bull. Amer. Meteor. Soc., 63, 1309–1313, 1982.

Willmott, C. J., and Matsuura, K.: Advantages of the mean absolute error (MAE) over the root mean square error (RMSE) in assessing average model performance, Climate Res., 30, 79-82, 10.3354/cr030079, 2005.

Wilson, K. B., Hanson, P. J., Mulholland, P. J., Baldocchi, D. D., and Wullschleger, S. D.: A comparison of methods for determining forest evapotranspiration and its components: sap-flow, soil water budget, eddy covariance and catchment water balance, Agric. For. Meteorol., 106, 153-168, 2001.

Yepez, E. A., Williams, D. G., Scott, R. L., and Lin, G.: Partitioning overstory and understory evapotranspiration in a semiarid savanna woodland from the isotopic composition of water vapor, Agric. For. Meteorol., 119, 53-68, 2003.

Yoo, J., Lee, D., Hong, J., and Kim, J.: Principles and Applications of Multi-Level H_2O/CO_2 Profile Measurement System, Korean J. Agric. For. Meteorol., 11, 27-38, 2009 (in Korean with English abstract).

Yuan, R., Kang, M, Park, S., Hong, J., Lee, D., and Kim, J.: The effect of coordinate rotation on the eddy covariance flux estimation in a hilly KoFlux forest catchment, Korean J. Agric. For. Meteorol., 9, 100-108, 2007.

Yuan, R., Kang, M., Park, S., Hong, J., Lee, D., and Kim, J.: Expansion of the planar-fit method to estimate flux over complex terrain, Meteorol. Atmos. Phys., 110, 123-133, 2011.
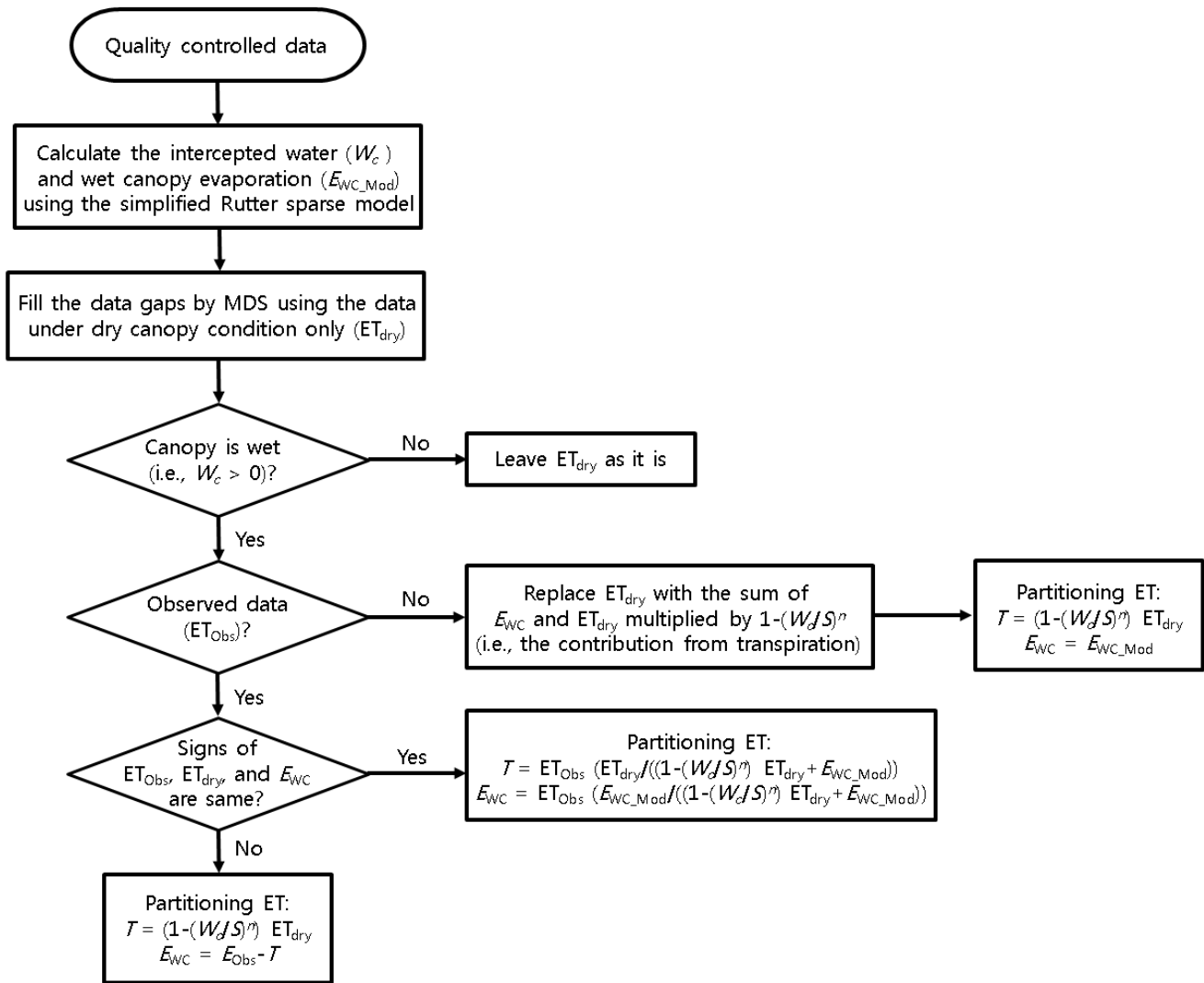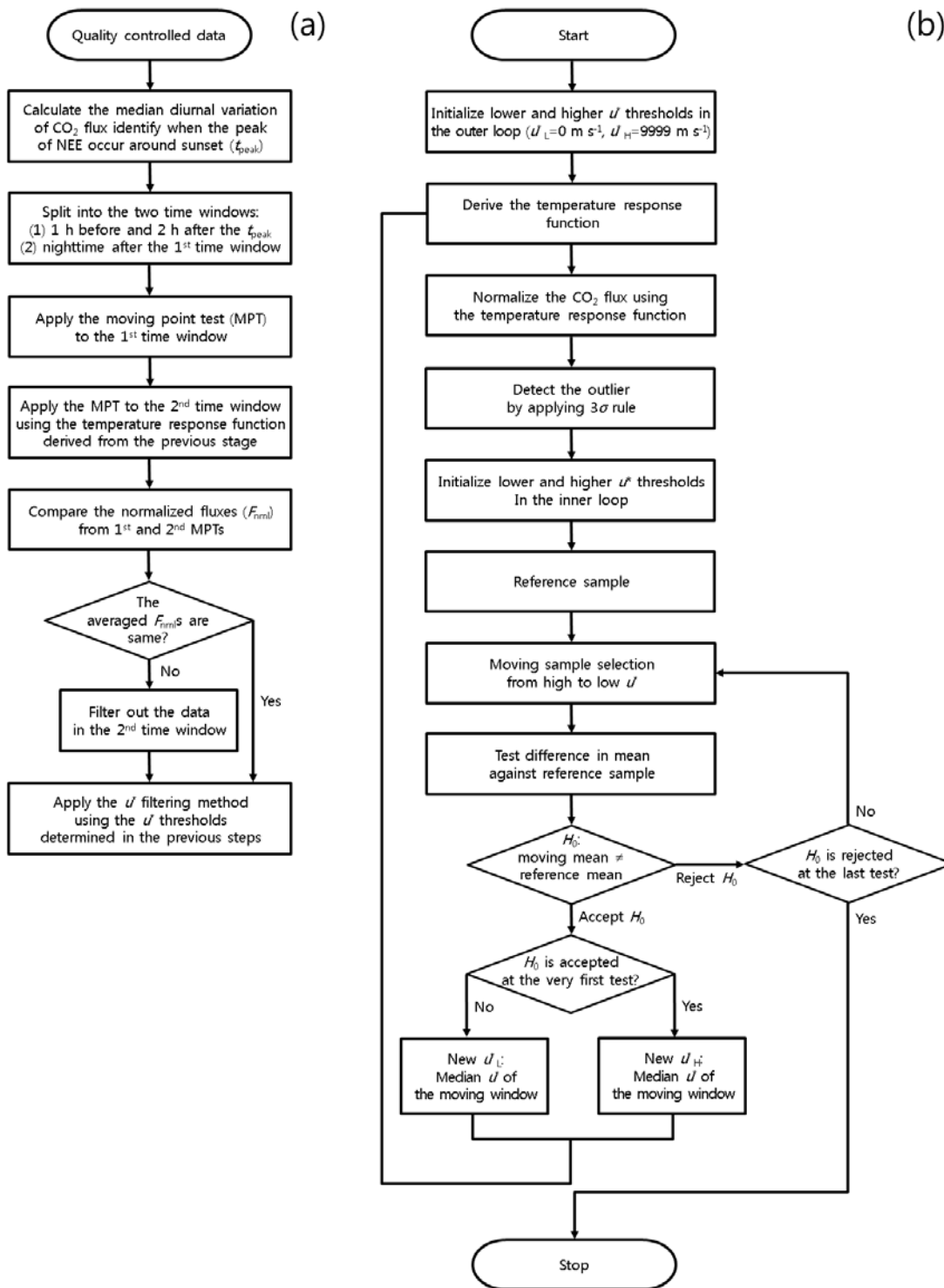
Quality controlled data

Calculate the intercepted water (W_c) and wet canopy evaporation (E_{WC_Mod}) using the simplified Rutter sparse model

Fill the data gaps by MDS using the data under dry canopy condition only (ET_{dry})

Canopy is wet (i.e., $W_c > 0$)? — No → Leave ET_{dry} as it is

Yes

Observed data (ET_{Obs})? — No → Replace ET_{dry} with the sum of E_{WC} and ET_{dry} multiplied by $1-(W_c/S)^n$ (i.e., the contribution from transpiration) → Partitioning ET:
$$T = (1-(W_c/S)^n)\ ET_{dry}$$
$$E_{WC} = E_{WC\_Mod}$$

Yes

Signs of ET_{Obs}, ET_{dry}, and E_{WC} are same? — Yes → Partitioning ET:
$$T = ET_{Obs}\ (ET_{dry}/((1-(W_c/S)^n)\ ET_{dry} + E_{WC\_Mod}))$$
$$E_{WC} = ET_{Obs}\ (E_{WC\_Mod}/((1-(W_c/S)^n)\ ET_{dry} + E_{WC\_Mod}))$$

No

Partitioning ET:
$$T = (1-(W_c/S)^n)\ ET_{dry}$$
$$E_{WC} = E_{Obs} - T$$

Figure 1: Flowchart of the gap-filling and partitioning technique for evapotranspiration.

(a)

- Quality controlled data
- Calculate the median diurnal variation of CO_2 flux identify when the peak of NEE occur around sunset (t_{peak})
- Split into the two time windows:
  (1) 1 h before and 2 h after the t_{peak}
  (2) nighttime after the 1st time window
- Apply the moving point test (MPT) to the 1st time window
- Apply the MPT to the 2nd time window using the temperature response function derived from the previous stage
- Compare the normalized fluxes (F_{nml}) from 1st and 2nd MPTs
- The averaged F_{nml}s are same?
  - No → Filter out the data in the 2nd time window
  - Yes
- Apply the u^* filtering method using the u^* thresholds determined in the previous steps

(b)

- Start
- Initialize lower and higher u^* thresholds in the outer loop ($u^*_L = 0$ m s^{-1}, $u^*_H = 9999$ m s^{-1})
- Derive the temperature response function
- Normalize the CO_2 flux using the temperature response function
- Detect the outlier by applying 3σ rule
- Initialize lower and higher u^* thresholds In the inner loop
- Reference sample
- Moving sample selection from high to low u^*
- Test difference in mean against reference sample
- H_0: moving mean ≠ reference mean
  - Reject H_0 → H_0 is rejected at the last test?
    - No → (back to Moving sample selection)
    - Yes → Stop
  - Accept H_0 → H_0 is accepted at the very first test?
    - No → New u^*_L: Median u^* of the moving window
    - Yes → New u^*_H: Median u^* of the moving window
- Stop

Figure 2: Flowcharts of the gap-filling and partitioning technique for CO_2 flux, the modified moving point test (MPT) method (a) and the original MPT (b; adapted from Gu et al. 2005).

22

Figure 3̶2: Comparison of the latent heat flux under (mostly) wet canopy condition (i.e., $W_c/S > 2/3$ where W_c is the intercepted canopy water and S is the canopy storage capacity) at the GDK (a) and GCK (b) sites: λET_{WC_Obs} indicates the observed latent heat flux under a wet canopy condition (λET_{WC}), while λET_{WC_MSH} indicates the estimated λET_{WC} ~~from~~ using the model-stats hybrid method. The dotted line represents the 1:1 line.
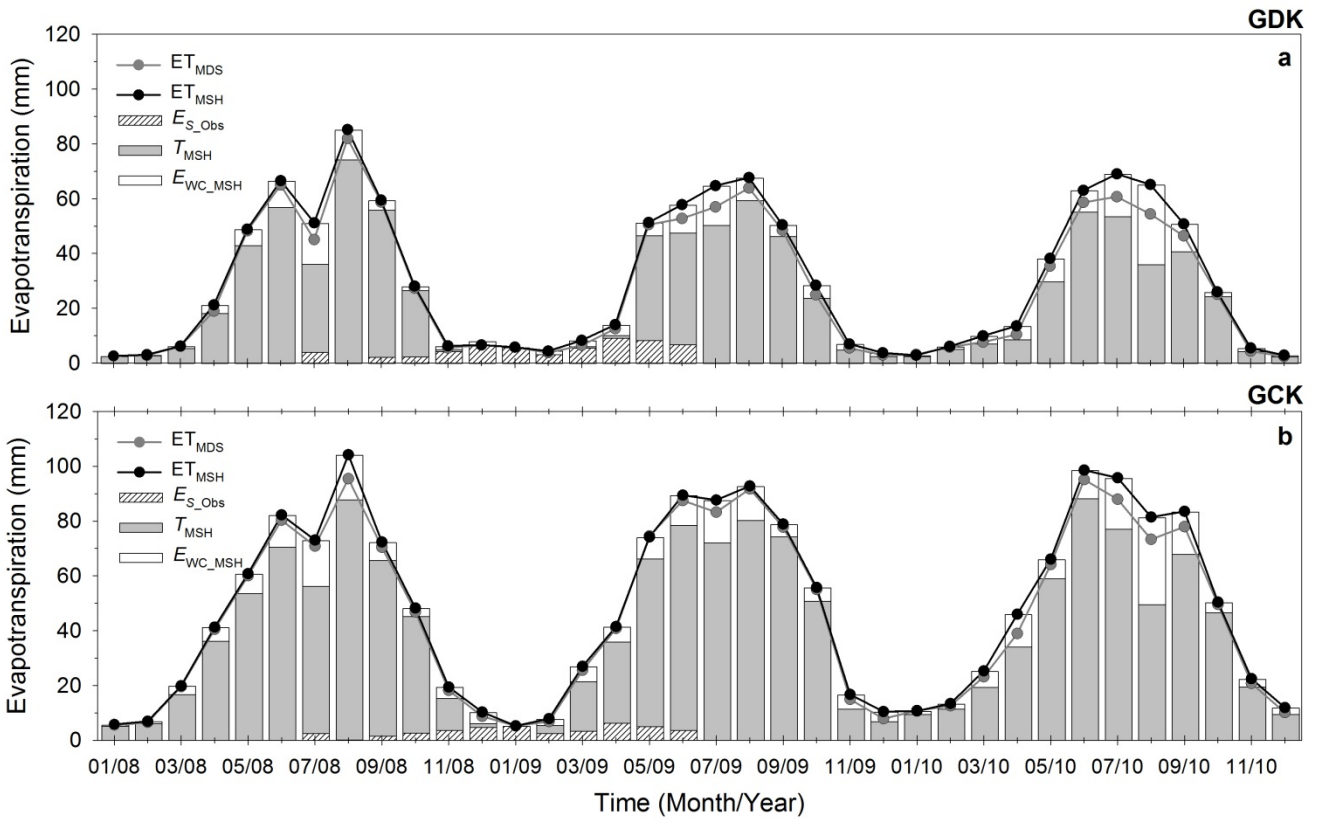
23

Figure 43: Seasonal variation of monthly integrated evapotranspiration (ET) with the gap-filled by the marginal distribution sampling method (ET$_{MDS}$); the ET gap-filled by the model-stats hybrid (MSH) method (ET$_{MSH}$), transpiration and wet canopy evaporation partitioned by the MSH method (T_{MSH} and E_{WC_MSH}), for the GDK (a) and GCK (b) sites. E_{S_Obs} indicates soil evaporation measured by the supplementary eddy covariance systems at the floors (adapted from Kang et al., 2009b).

24
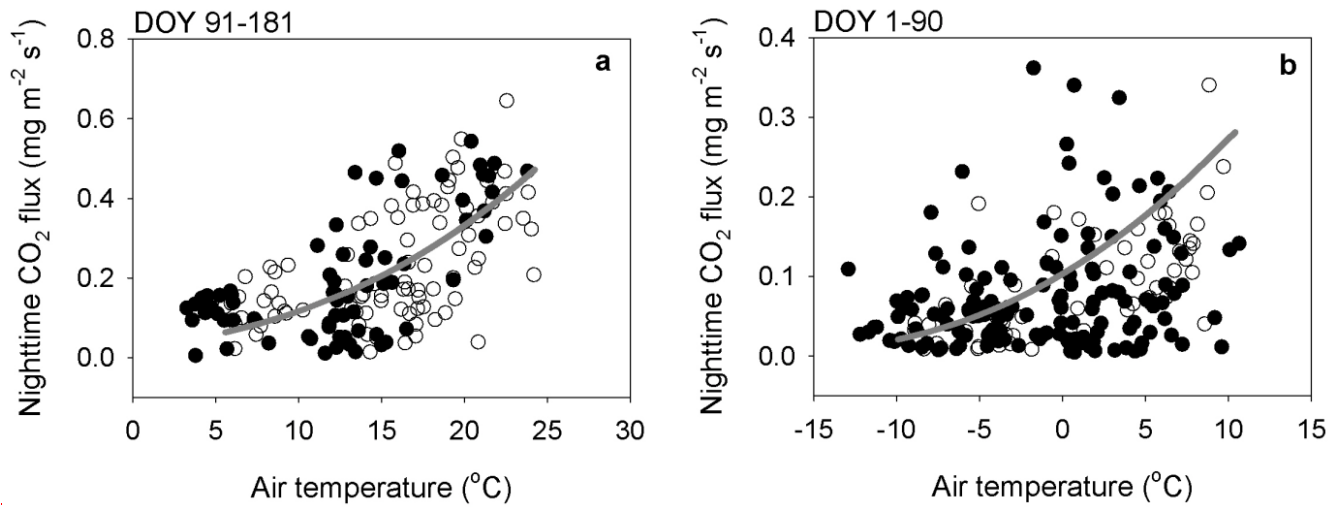
Figure 5: The relationship between the nighttime CO_2 flux and air temperature after applying the modified moving point test (MPT) (filtered by the u^* thresholds which are determined from the modified MPT) for the GCK in 2008, DOY 91-181 (a) and DOY 1-90 (b). The white color indicates the 1st time window, whereas black color indicates the 2nd time window. The solid line indicates the fitting line of Lloyd-Taylor equation using the filtered data of the 1st time window.
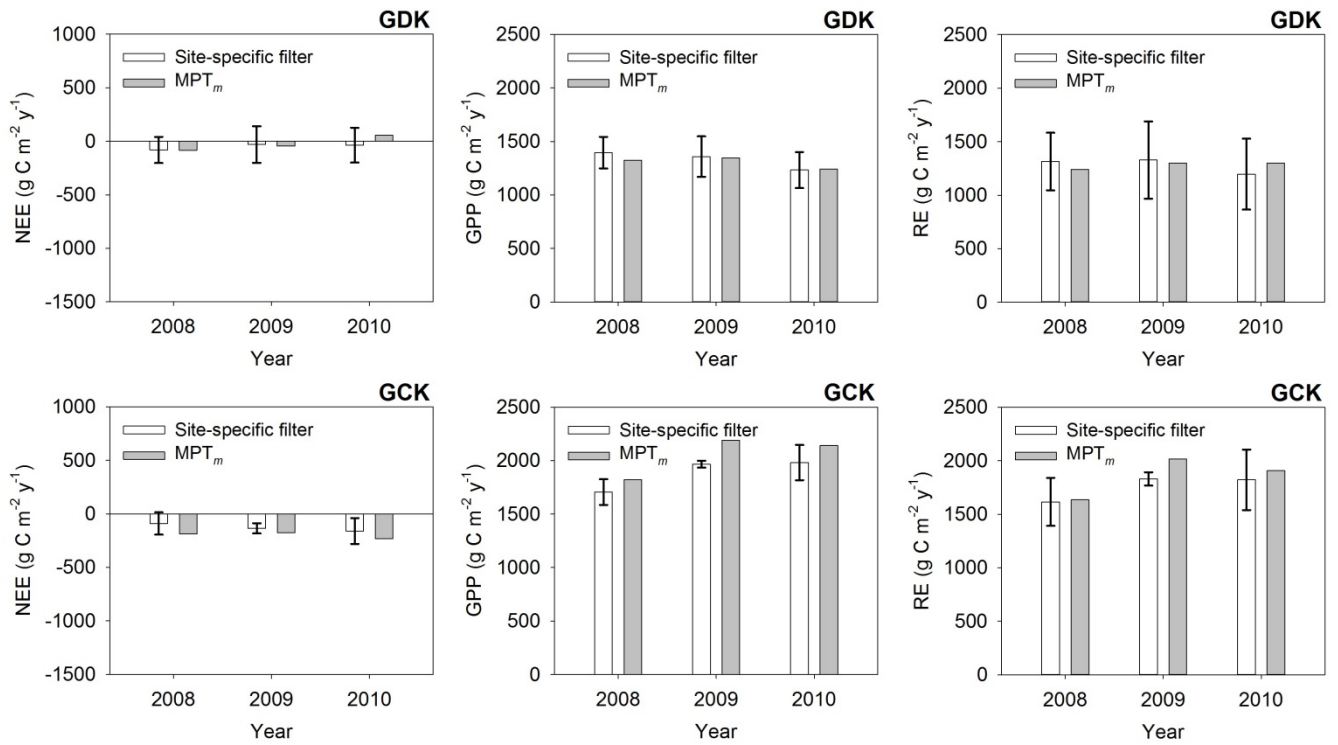
Figure 6: The (averaged) annual CO_2 budget (NEE: net ecosystem exchange, GPP: gross primary production, RE: ecosystem respiration) from the three general nighttime correction methods (i.e., u^* filtering method, light response curve method, and van Gorsel method) after applying the site-specific filter (adapted from Kang et al., 2017) and that from the modified MPT method for the sites. Error bar indicates the standard deviation of the results from the three general nighttime correction methods.

5
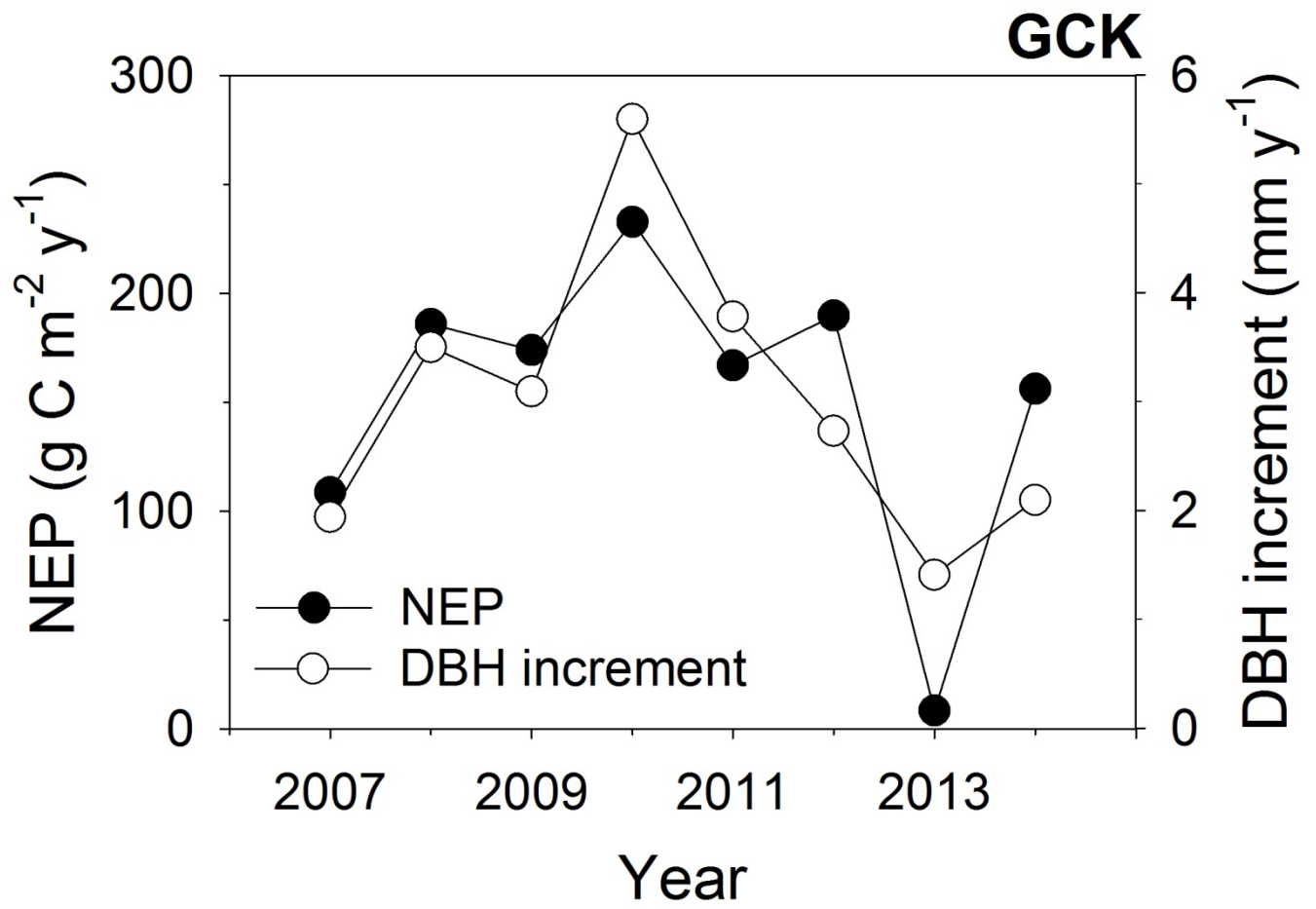
Figure 7: The interannual variabilities of the annual net ecosystem production and the annual increment of DBH (diameter at breast height) for the GCK site.
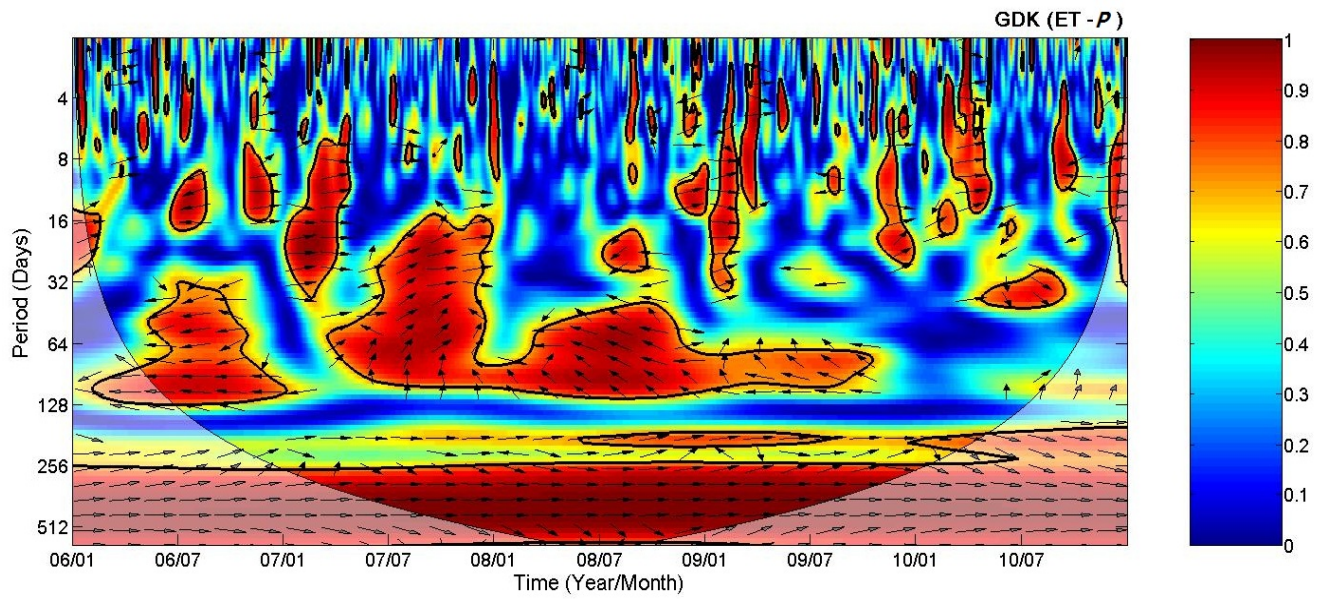
Figure 84: Wavelet coherence spectrum of evapotranspiration (ET) with rainfall (*P*) for the GDK site. A thick solid contour is the 5% significance level against red noise as calculated from a Monte Carlo simulation. Arrows are the relative phase angle (with in-phase (positive correlation) pointing right, antiphase (negative correlation) pointing left, and *P* leading ET by 90° pointing straight down). The shaded area indicates the cone of influence where the edge effects might distort the results.

Table 1: Statistical parameters for the error assessment at the study sites. MBE, MAE, RMSE, and _d_ indicate mean bias error, mean absolute error, root mean square error, and index of agreement, respectively. Slope and _r²_ are from the linear regression analysis.

		No. of data	MBE	MAE	RMSE	d	Slope	r^2
		--	$W\ m^{-2}$	$W\ m^{-2}$	$W\ m^{-2}$	--	--	--
GDK	2008	333	6	20	30	0.93	0.80	0.72
	2009	222	12	21	39	0.91	1.10	0.73
	2010	215	14	23	34	0.90	1.00	0.63
GCK	2008	318	-4	23	36	0.95	0.84	0.83
	2009	246	-10	26	44	0.94	0.85	0.79
	2010	285	7	24	39	0.95	0.97	0.82

5

Table 2: Summary results generated from the modified moving point test (MPT) for the GDK and GCK sites. u_L^* and u_H^* indicate lower and higher u^* thresholds, 1st and 2nd indicate the 1st and 2nd time windows, respectively.

Site	Year	DOY	u_L^* 1st	u_H^* 1st	u_L^* 2nd	u_H^* 2nd	Drainage effect
GDK	2008	1-90	0.179	9999	0.337	9999	negligible
		91-181	0.215	9999	0.363	9999	significant
		182-273	0.178	9999	0.215	9999	negligible
		274-366	0.144	0.271	0.171	9999	negligible
	2009	1-90	0.216	9999	0.411	9999	negligible
		91-181	0.406	9999	0.169	9999	significant
		182-273	0.238	9999	0.156	9999	significant
		274-365	0.338	9999	0.184	0.506	significant
	2010	1-90	0	9999	0.326	0.47	negligible
		91-181	0	9999	0.202	0.341	significant
		182-273	0.247	9999	0.173	9999	negligible
		274-365	0.166	9999	0.255	9999	negligible
GCK	2008	1-90	0.409	9999	0.174	9999	significant
		91-181	0.29	9999	0.25	9999	negligible
		182-273	0.164	9999	0.221	9999	negligible
		274-366	0.149	9999	0.197	9999	negligible
	2009	1-90	0.248	9999	0.425	9999	negligible
		91-181	0.252	9999	0.122	9999	significant
		182-273	0.171	9999	0.141	0.198	significant
		274-365	0.232	9999	0.238	9999	negligible
	2010	1-90	0.157	9999	0.295	9999	significant
		91-181	0.157	9999	0.137	9999	significant
		182-273	0.125	9999	0.122	0.216	significant
		274-365	0.098	0.417	0.348	9999	significant

Table 32: The annual CO_2 and H_2O budget (NEE: net ecosystem exchange, GPP: gross primary production, RE: ecosystem respiration, ET: evapotranspiration, E_{WC}: wet canopy evaporation) and water use efficiency at the ecosystem-level (WUE_{Eco}) and the canopy-level (WUE_{Canopy}) for the study sites.

		NEE	GPP	RE	ET	E_{WC}	WUE_{Eco}	WUE_{Canopy}
		g C m^{-2} y^{-1}	g C m^{-2} y^{-1}	g C m^{-2} y^{-1}	mm	mm	g C·(kg H_2O)$^{-1}$	g C·(kg H_2O)$^{-1}$
	2006	-114	1,149	1,035	361	66	0.32	2.17
	2007	-14	1,183	1,169	398	116	0.03	2.42
GDK	2008	-84	1,326	1,242	383	53	0.22	2.20
	2009	-45	1,346	1,301	360	56	0.12	2.45
	2010	58	1,242	1,300	353	82	-0.16	2.59
	2007	-109	1,892	1,783	557	122	0.20	2.16
GCK	2008	-186	1,822	1,636	544	78	0.34	1.93
	2009	-174	2,190	2,016	587	77	0.30	2.12
	2010	-233	2,140	1,907	606	112	0.38	2.15

5

Appendix A: The differences in annual budgets of CO_2, latent, and sensible heat fluxes depending on the estimations of storage terms

To estimate net ecosystem exchange (NEE) for a target ecosystem using eddy covariance technique, particularly for forests, we should consider not only the eddy flux term but also the storage term, i.e., the change of stored mass and energy of the air in the control volume. Particularly, the storage terms make a large contribution to total NEE under calm condition (i.e., weak turbulence condition). The storage term of carbon dioxide (CO_2) was calculated as follows (e.g., Aubinet et al., 2001; Papale et al., 2006):

$$S_c = -\int_0^h \frac{P_a(z)}{R \cdot T_a(z)} \frac{\partial c(z)}{\partial t} dz$$

(A1)

where S_c is the storage term of CO_2 (μmol m^{-2} s^{-1}), P_a is the barometric pressure (kPa), R is the gas constant (8.314×10^{-3} kPa m^3 K^{-1} mol^{-1}), c is the CO_2 concentration (μmol mol^{-1}), z is height (m), t is time (s), and h is the height of the control volume (usually, the height of the eddy covariance system). The storage terms of water vapor (H_2O) and heat are also calculated similarly to Eq. (4). The eight-level vertical profile systems for CO_2, H_2O, and air temperature are operated at the GDK and GCK sites (Yoo et al., 2009). The storage terms are calculated by finite difference method using the data from profile system. If profile system is not installed or is not operated normally, the storage terms are calculated using the data from eddy covariance system (i.e., considering single level scalar variation only) under the assumption that the concentrations and air temperature are constant with height (Papale et al. 2006). Such calculated storage terms of CO_2, H_2O, and air temperature are added to those eddy covariance terms for estimating those NEEs.

Table A1 shows the differences in annual budgets of CO_2 flux / evapotranspiration (ET) / sensible heat flux (*H*) among the estimations of storage terms for the study sites in 2008. The most notable result is that the CO_2 budgets, i.e., the NEE, gross primary production (GPP), and ecosystem respiration (RE) show the large differences among the estimations of storage terms. Meanwhile, the ET and *H* budgets are approximately identical without regard to the estimations of storage terms. The main reason of the minor effect of the storage term estimation in ET and *H* is that the fluxes are always very low at night, when the storage term is important. As the other possible causes, CO_2 is heavier than air, and significant source and sink exist at various levels (e.g., soil, canopy) that are unlikely ET and *H*. For the CO_2 budgets, the more correctly the storage terms were estimated, the larger the NEE (i.e., stronger carbon sink), GPP, and RE are quantified primarily due to the underestimation of nighttime CO_2 fluxes (i.e., RE). Especially if the storage terms are not considered, there were large differences compared to the cases of considering the storage terms using any approach. Such results suggest that we should measure and process more systematically and accurately not only the eddy flux term but also the storage term for quantifying NEE for the forest ecosystem.

		NEE	GPP	RE	ET	*H*
			$g\,C\,m^{-2}\,y^{-1}$		$mm\,y^{-1}$	$MJ\,m^{-2}\,y^{-1}$
			MDS & MPT$_m$		MDS	
GDK	Profile	-129	1,297	1,169	367	605
	Single	-181	1,209	1,028	365	604
	No storage	-266	940	674	363	605
GCK	Profile	-147	1,614	1,467	533	1,085
	Single	-224	1,539	1,315	533	1,085
	No storage	-290	1,280	990	527	1,092

Appendix AB: Parameterizations of canopy storage

The rainfall interception is sensitive to the change of canopy storage capacity (*S*) and vegetation fraction (σ_f i.e., 1-gap fraction) (e.g., Shi et al., 2010). One of the characteristics common among the temperate forests considered in this study is a dense canopy. It means that the vegetation fractions in the forests are close to 1 (except before leaf unfolding and after leaf fall periods). Moreover, the gap fraction can be measured using a plant canopy analyzer with relative ease. Therefore, the error of the result from the model is mostly derived from the parameterization of *S* (see Appendix BC for more detailed information). The canopy storage capacity is affected by not only leaf area but also the other factors such as leaf shape, leaf angle, leaf/shoot clumping and hydrophobicity (water repellency) of a leaf (e.g., Crockford and Richardson, 2000). Additionally, the relationships between *S* and these characteristics are changeable according to meteorological conditions (e.g., the wind, rainfall intensity), which make the parameterization of *S* difficult (e.g., Dunkerley, 2009). Therefore, we used the simple parameterization of *S* of VIC LSM (i.e., $S = K_L \times$ leaf (or plant) area index, where $K_L = 0.2$; Liang et al., 1994) and evaluated whether the parameterization was reasonable or not. The relationships between the leaf area index (LAI) and *S* in the previous studies are presented in Fig. AB1, indicating that the parameterization in VIC LSM (i.e., $K_L = 0.2$) is reasonable and the K_L ranges from 0.1 to 0.3. Further studies on the parameterization of *S* using leaf structure (e.g., leaf shape, leaf angle, leaf/shoot clumping) would be worth conducting for more accurate estimation of wet canopy evaporation.
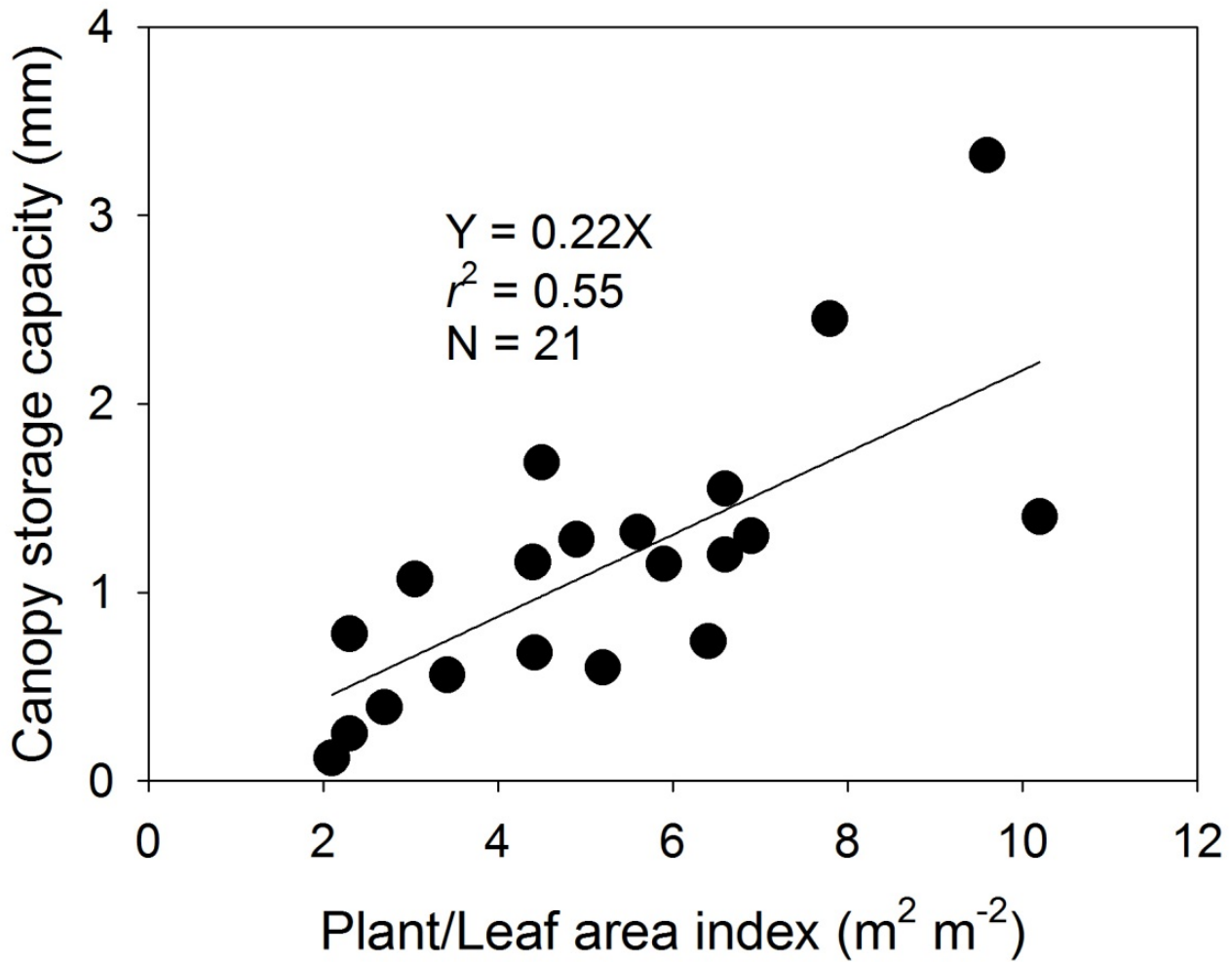
Figure AB1: Relationship between canopy storage capacity and plant/leaf area index (the data obtained from Table AB1).

Table AB1: Review of the canopy storage capacity for wet canopy evaporation modeling in the previous studies.

Vegetation type	Species	Country	Longitude /Latitude	Canopy storage capacity (mm)	Plant/Leaf area index (m^2 m^{-2})	Density (trees ha^{-1})	References
Laurel forest	*Myrica faya Ait., Laurus azorica(Seub.) Franco, Persea indica (L.) Spreng, Ericaarborea L., Ilex perado ssp. plathyphylla Webb & Amarra, Ilex canariensis Poivet*	Spain	28°27′N, 16°24′W	2.45	7.8	1,693	Aboal et al. (1999)
Pine-oak forests	*Pinus pseudostrobus, Q.canbyi, Q.laeta*	Mexico	24°42.3′N, 99°52.2′W	0.78	2.3	819	Carlyle-Moses and Price (2007)
Mixed agricultural cropping system	*Manihot esculenta Crantz, Zeamays L., Oryza sativa L.*	Indonesia	7°03′S, 108°04′W	0.12	2.1		van Dijk and Bruijnzeel (2001)
Plantation forest of Maritime pine	*Pinus pinaster Ait.*	France	44°5′N, 0°5′W	0.25	2.3	430	Gash et al. (1995)
Norway spruce and Scots pine	*Picea abies (L.) Karst., Pinus sylvestris (L.)*	Sweden	60°5′N, 17°29′E	1.69	4.5		Lankreijer et al. (1999)
Secondary broad leaved deciduous forests	*Quercus serrara, Clethra barbinervis*	Japan	35°02′N, 137°11′E	1.07	3.05		Deguchi et al. (2006)
Mature rain forests		Colombian Amazonia		1.16	4.4		Marin et al. (2000)
				1.28	4.9		
				1.32	5.6		
				1.55	6.6		
Tabonuco type forest	*Dacryodes excelsa*	Puerto Rico	18°18N, 65°5′W	1.15	5.9		Schellekens et al. (1999)
Mixed White Oak Forest	*Quercus serrata Thunb., Sasa paniculata Makino et Shibata.*	Japan	35°19′N, 133°35′E	0.6	5.2		Silva and Okumura (1996)
Secondary broad-leaved deciduous forests(Summer)		Japan		0.68	4.42		Park (2000)
Secondary broad-leaved				0.39	2.7		

deciduous forests(Winter)						
Secondary broad-leaved deciduous forests (Summer)				0.74	6.41	
Secondary broad-leaved deciduous forests (Winter)				0.39	3.42	
Douglas-fir forest (Young)		USA	45°49.1′N, 121°59.7′W	1.4	10.2	Pypker et al. (2005)
Douglas-fir forest (Old)			45°49.2′N, 121°54.1′W	3.32	9.6	
Decidous mixed forest (South)	*Carpinusorientalis croaticus, Quercus pubescentis*	Slovenia		1.2	6.6	Sraj et al., (2008)
Deciduous mixed forest (North)	*F. ornus, Q. pubescentis*			1.3	6.9	

36

Appendix BC: Sensitivity test and parameter optimization of the wet canopy evaporation model

In the simplified Rutter sparse model (Liang et al., 1994), there are many parameters (e.g., σ_f, S, n, r_a, and r_0) for estimating the wet canopy evaporation (E_{WC}) and the intercepted canopy water (W_c). Since the model results may be sensitive to the parameters and the parameters may be site-specific, the parameter optimization using available flux data under wet canopy condition should be accompanied for the generalization of the model. Considering that the gap-filling and partitioning are a kind of interpolation and extrapolation (i.e., identifying relationships between a target flux and its drivers, and interpolating and extrapolating the relationships), it is an appropriate strategy for the gap-filling and partitioning of evapotranspiration using the model.

First, we conducted a sensitivity test of the model to the parameters (i.e., k, K_L, n, and r_0) using the dataset in 2008

10 (Change in E_{WC} (%) $= \dfrac{E_{WC\_perturb} - E_{WC\_default}}{E_{WC\_default}} \times 100$, $E_{WC\_default}$: Annually integrated E_{WC} simulated with default

parameters, $E_{WC\_perturb}$: Annually integrated E_{WC} simulated after a change in each parameter. Only one parameter is changed one at a time, while other parameters are held in constants, e.g., Shi et al., 2010). Before testing the sensitivity, we set the lower/upper boundaries (and default values) based on the literature reviews: $k = 0.3 \sim 1.5$ (Jones, 2013; The default values of k are 0.75 and 0.485 for the GDK and GCK, respectively. Those values were obtained from the actual measurement using a plant canopy analyzer (Model LAI-2000; Li-Cor Inc.)); $K_L = 0.1 \sim 0.3$ (see Appendix B; The default values of K_L is 0.2 (Dickinson, 1984).); $n = 0.5 \sim 1$ (Chen and Dudhia, 2001; Liang et al., 1994; Valente et al., 1997; The default values of n is 2/3 (Deardorff, 1978).); $r_0 = 0$ (for short vegetation) ~ 2 s m^{-1} (for tall vegetation) (Perrier, 1975; Rana et al., 1993; The default values of r_0 is 2 (Perrier, 1975).). K_L is the most influential parameters (Fig. BC1), implying that we should take great care to minimize parameter estimation error for K_L.

20 Using a small number of the observed latent heat flux data under wet canopy condition (when $W_c/S > 2/3$) from 2008 to 2010, we optimized the parameters except k (because we obtained the k from the actual measurement) towards minimizing the root mean square error of the method (using the bound constrained optimization code in MATLAB®, "fminsearchbnd." http://kr.mathworks.com/matlabcentral/fileexchange/8277-fminsearchbnd--fminsearchcon). We randomly divided the available dataset into the datasets for parameter optimization and validation (i.e., validation after optimization). The ratio of

25 the optimization-validation datasets was arbitrarily set to 7:3. Table BC1 shows the model parameters and the statistical parameters for the error assessment before and after the parameter optimization. After the optimization, the parameters slightly changed from the default values. However, we still used the default values conservatively since the model results from before and after the optimization were not statistically different in the error assessment.
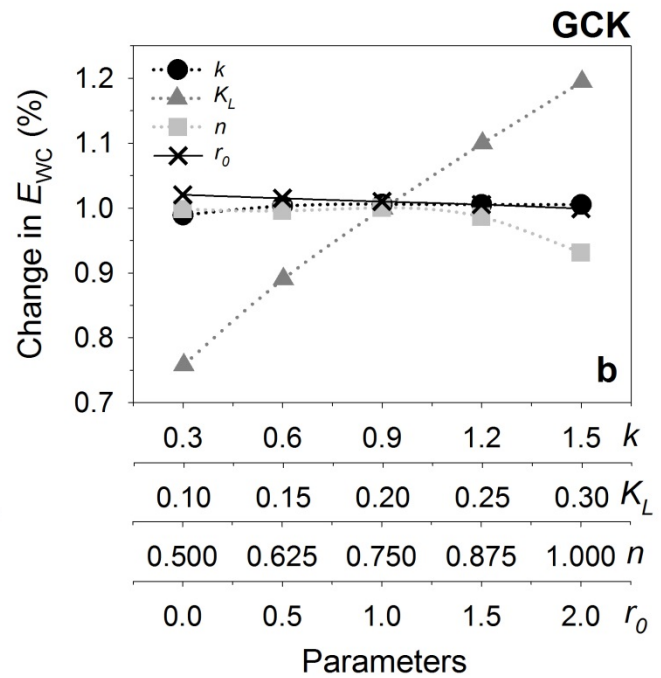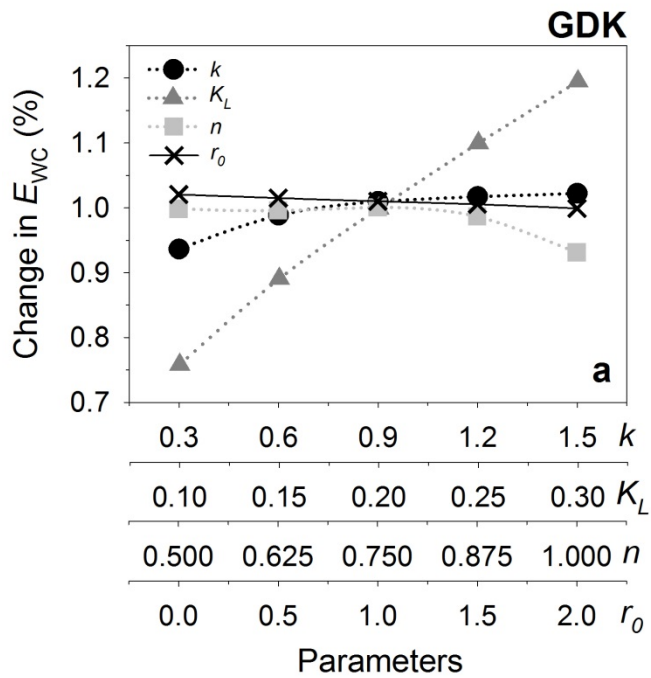
37

Figure BC1: Sensitivity test of the wet canopy evaporation model to the parameters (i.e., k, K_L, n, and r_0).

Table BC1: Statistical parameters before and after the parameter optimization for the error assessment at the study sites. MBE, MAE, RMSE, and d indicate mean bias error, mean absolute error, root mean square error, and index of agreement, respectively. Slope and r^2 are from the linear regression analysis. The default values of K_L, n, and r_0 were 0.2 (0.2), 2/3 (2/3), and 2 (2) for the GDK (GCK), respectively. After the optimization, those values changed to 0.1966 (0.2314), 0.7279 (0.6930), and 2 (2) for the GDK (GCK), respectively.

			MBE	MAE	RMSE	d	Slope	r^2
			$W\ m^{-2}$	$W\ m^{-2}$	$W\ m^{-2}$	--	--	--
GDK	Optimization dataset ($N = 538$)	before optim.	10	22	36	0.91	0.93	0.67
		after optim.	10	22	36	0.91	0.92	0.66
	Validation dataset ($N = 232$)	before optim.	10	19	29	0.93	0.96	0.73
		after optim.	10	19	29	0.93	0.96	0.73
GCK	Optimization dataset ($N = 593$)	before optim.	-2	24	41	0.95	0.89	0.81
		after optim.	-2	24	41	0.95	0.90	0.81
	Validation dataset ($N = 256$)	before optim.	-1	24	38	0.95	0.87	0.81
		after optim.	-1	24	38	0.95	0.88	0.81

Appendix C: Further evaluation of the MSH using a closed-path EC system

For further evaluation of the model-stats hybrid (MSH) method, we conducted a commercialized closed-path infrared gas analyzer with the heated tube (Model EC155, Campbell Scientific Inc., Logan, Utah, USA) from August 18, 2015 to October 25, 2015 for the GDK site. The open- and closed- path gas analyzers shared the one sonic anemometer. We applied the MSH to the latent heat fluxes (λET) from the open-path eddy covariance (EC) system for gap-filling the λET under wet canopy condition, and the frequency response correction (Fratini et al., 2012) to the λET from the closed-path EC system for correcting the tube attenuation effect especially under high relative humidity (RH) condition. Then, we compared the λET (mostly) wet canopy conditions (λET_{WC}, i.e., λET when $W_c/S>2/3$) from the MSH ($\lambda ET_{WC\_MSH\_OP}$) against the observed λET_{WC} from the closed-path EC system ($\lambda ET_{WC\_Obs\_CP}$) similar to the Chapter 3.1 (Fig. C1).

Before the comparison, it should be noted that the data retrieval rate under wet canopy condition of the closed-path EC system was 50% higher than that of the open-path EC system, however, there were still missing data for the considerable period despite the closed-path gas analyzer was conducted. The missing was mainly caused by the malfunction of the sonic anemometer and the unsatisfactory conditions for EC measurement (e.g., nonstationary and unfavorable turbulent developed conditions). The results of the error assessment (i.e., 10 W m^{-2} of MBE, 19 W m^{-2} of MAE, 29 W m^{-2} of RMSE, 0.90 of d, 1.04 of Slope, 0.68 of r^2) were within the ranges of those from the comparison between the $\lambda ET_{WC\_MSH\_OP}$ and the λET_{WC_Obs} in the Chapter 3.1 (i.e., the case of the open-path EC system). Overall, such results imply the robustness of the MSH method as well as the necessity of appropriate λET_{WC} gap-filling method (e.g., MSH) in the case of the measurement using a closed-path EC system, like the case of an open-path EC system.
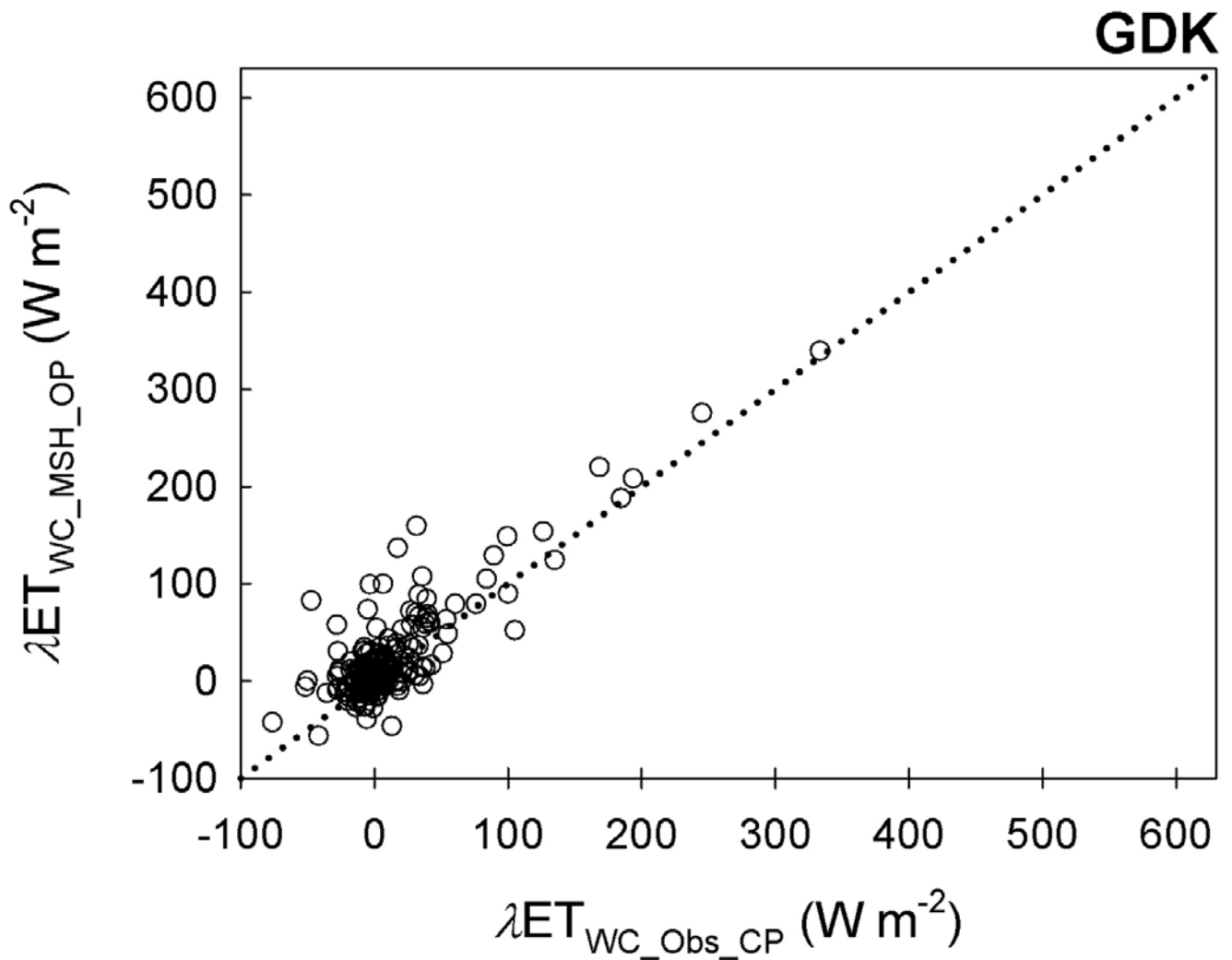
Figure C1: Comparison of the latent heat flux under (mostly) wet canopy condition (i.e., $W_c/S > 2/3$ where W_c is the intercepted canopy water and S is the canopy storage capacity) at the GDK site: $\lambda ET_{WC\_Obs\_CP}$ indicates the observed latent heat flux under a wet canopy condition (λET_{WC}) from a closed-path eddy covariance (EC) system, while $\lambda ET_{WC\_MSH\_OP}$ indicates the estimated λET_{WC} from an open-path EC system using the model-stats hybrid method. The dotted line represents the 1:1 line.

Appendix D: Modified van Gorsel method

The detailed procedure for selecting the observed nighttime CO_2 flux which can represent the actual RE for hilly terrain is proposed by van Gorsel et al. (2009) as follows (the VGF method): (1) calculate the mean diurnal variation of the observed CO_2 flux (F_{CO2_Obs}) for a certain period (e.g., 30 days), and identify when the peak of F_{CO2_Obs} occurs approximately at sunset, (2) extract F_{CO2_Obs}s one or two hours before and after the time of peak occurrence, (3) exclude the data among the extracted if it rains, or the atmosphere is stable, or the fluctuation of F_{CO2_Obs} is high, or F_{CO2_Obs} exceed a certain range, and (4) apply the nighttime correction using the remains. van Gorsel et al. (2009) argued that the RE from the light response curve method (RE_{LRC}) can be appropriate criteria for judging abnormal values, and excluded the data, which is smaller than 50% of averaged RE_{LRC} or larger than 200% of that. Notably, they changed the width of the range (e.g., minimum of 50% and a maximum of 200% to a minimum of 25% and a maximum of 400%) which may be subjective, and confirmed that the results are statistically the same within a 95% confidence interval. However, we discerned that if the result from light response curve method is excessively under/overestimated, the method proposed by van Gorsel et al. (2009) can be affected by the result. Specifically, the result of the nighttime NEE correction is not sensitive to the width of the range, which is used for data filtering criteria, but may be sensitive to the center of the range (i.e., the value of RE_{LRC}).

Therefore, we modify the peak values of mean diurnal variation are directly used to estimate the parameters in the RE function (i.e., Lloyd Taylor equation) based on the basic idea of the VGF method as follows: (1) instead of the mean diurnal variation, use the median diurnal variation which is less affected by the outliers, (2) calculate the median air temperature at the time of peak RE occurrences for the same period, (3) shift the window to calculate the median diurnal variation daily, obtain a sufficient dataset of RE and air temperature (maximum of 30 pairs) for estimating R_{ref} and E_0 in the Lloyd Taylor equation. This method can be applied independently (RE_{LRC} is not necessary). We call the method the 'modified van Gorsel method (VGF_m).' This VGF_m method produces similar results to the original VGF method (with dissimilarity during the monsoon season, which is probably caused by the low data retrieval rate at that time), which supports that the VGF_m method is a good alternative to original VGF method (Fig. D1).
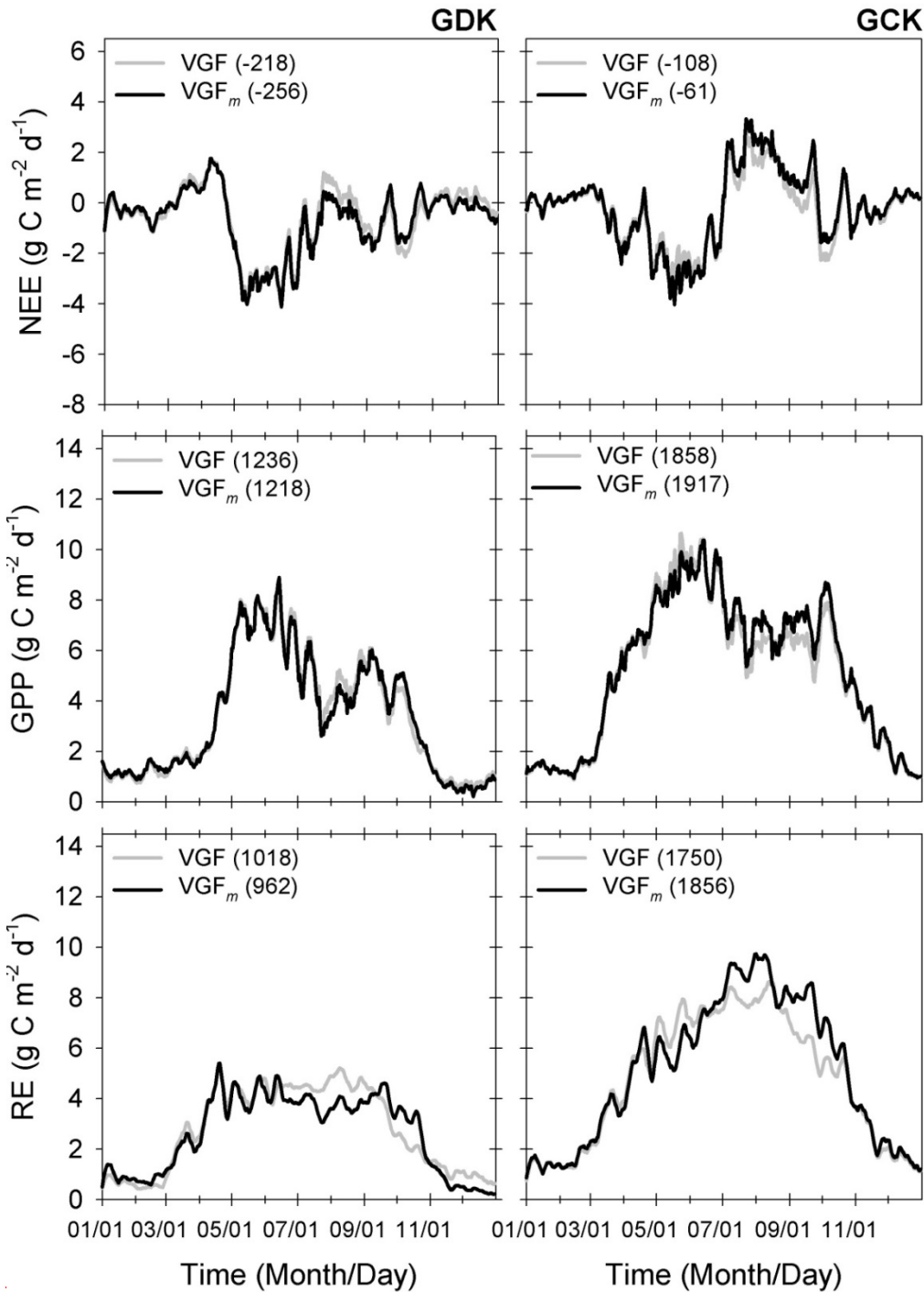
42

Appendix DE: Error assessment

In order to evaluate the latent heat flux under wet canopy condition obtained from the model-stats hybrid method, we compared them against the observed data using four statistical measures, following Willmott and Matsuura (2005). Mean bias error (MBE) is the average of the residuals. Mean absolute error (MAE) is the average of the absolute values of the residuals. A large deviation from zero implies that the estimation generally overestimates or underestimates compared to the observed values. We also considered root mean squared error (RMSE) which is often reported with MAE because RMSE is more sensitive to large errors than MAE.

$$\text{MBE} = \sum \frac{Y_{est} - Y_{obs}}{n} \qquad \text{(DE1)}$$

$$\text{MAE} = \sum \frac{\left| Y_{est} - Y_{obs} \right|}{n} \qquad \text{(DE2)}$$

$$\text{RMSE} = \sqrt{\sum \frac{(Y_{est} - Y_{obs})^2}{n}} \qquad \text{(DE3)}$$

MBE, MAE, and RMSE give estimates of the average error, but none of them provides information about the relative size of the average difference. Thus, we further considered an additional index of agreements (d), following Willmott (1982):

$$d = 1 - \left[\frac{\sum (Y_{est} - Y_{obs})^2}{\sum (\left| Y_{est}' \right| + \left| Y_{obs}' \right|)^2} \right] \qquad \text{(DE4)}$$

where $Y_{est}' = Y_{est} - \overline{Y_{obs}}$ and $Y_{obs}' = Y_{obs} - \overline{Y_{obs}}$ (where overbar is an averaging operator). It ranges from 0 to 1, where 0 is for complete disagreement and 1 for complete agreement between the observation and the estimates. It is both a relative and bounded measure that can be widely applied in order to make cross-comparison between models.